Self-consistent treatment of the quark condensate and hadrons in nuclear matter

E.G.Drukarev, M.G.Ryskin, V.A.Sadovnikova

Petersburg Nuclear Physics Institute, Gatchina, St.Petersburg 188350, Russia e-mail: drukarev@thd.pnpi.spb.ru, ryskin@thd.pnpi.spb.ru, sadovnik@thd.pnpi.spb.ru

Abstract

We calculate the contribution of pions to the $\bar{q}q$ -expectation value $\kappa(\rho)=< M|\bar{q}q|M>$ in symmetric nuclear matter. We employ exact pion propagator renormalized by nucleon-hole and isobar-hole excitations. Conventional straightforward calculation leads to the "pion condensation" at unrealistically small values of densities, causing even earlier restoration of chiral symmetry. This requires a self-consistent approach, consisting in using the models, which include direct dependence of in-medium mass values on $\kappa(\rho)$, e.g. the Nambu–Jona-Lasinio–model. We show, that in the self-consistent approach the ρ -dependence of the condensate is described by a smooth curve. The "pion condensate" point is removed to much higher values of density. The chiral restoration does not take place at least while $\rho < 2.8\rho_0$ with ρ_0 being the saturation value. Validity of our approach is limited by possible accumulation of heavier baryons (delta isobars) in the ground state of nuclear matter. For the value of effective nucleon mass at the saturation density we found $m^*(\rho_0) = 0.6m$, consistent with nowadays results of other authors.

PACS. 13.75.Gx Pion-baryon interactions; 24.80.+y Nuclear tests of fundamental interactions and symmetries; 24.85.+p Quarks, gluons, and QCD in nuclei and nuclear processes

1 Introduction

In this paper we present the calculation of density dependence of the scalar quark condensate $\kappa = \langle M|\bar{q}q|M \rangle$ in symmetric nuclear matter. The gas approximation [1] provides linear dependence, while account of interactions in medium leads to nonlinear contributions. Although at normal density ρ_0 the nonlinear corrections are rather small [1] — [11], it is interesting to follow their behaviour while the density increases.

We show, that the main contribution to nonlinear terms comes from the interaction of the scalar quark operator with the pion cloud. Thus we must average the operator $\bar{q}q$ over in-medium pions.

Concrete calculation are carried out by use of Feynman diagram technique (Fig. 1) with the pions described by propagators, renormalized by interactions with medium. The propagation of pions in medium is a special story, related closely to the problem of pion condensation [12], [13]. The key point of the latter phenomena is that a solution of dispersion equation with negative frequency squared, $\omega_c^2 < 0$ emerges at certain value ρ_c . This signals the change in the structure of the ground state. The general belief is that the phenomena does not take place up to the values of about twice the normal density.

We show that the pion condensation is related to the appearance of a new branch of the solutions of pion dispersion equation on the physical sheet of pion frequencies, besides the well-known branches with pion quantum numbers (these are the pion, isobar and sound branches).

Account of the condensation singularity in the calculation of $\kappa = \langle M|\bar{q}q|M\rangle$ leads to important physical consequence: the value of κ turns to zero at the density values smaller than ρ_c . Thus, while the density increases, the chiral phase transition takes place earlier, than the pion condensation does.

We show that the value of the critical density ρ_c (and thus, the value of the density of the chiral phase transition) depends strongly on the magnitude of the effective nucleon mass m^* in medium. This happens because the pion polarization operator Π is proportional to m^* , thus entering the dispersion equation and propagator. The effective mass m^* decreases while the density increases. The decrease of $m^*(\rho)$ causes the diminution of the polarization operator reflecting the weakening of the medium influence on the pions. This results in a shift of the point of the pion condensation to a larger density.

However, assuming any of conventional nuclear physics equations for in-medium mass m^* with direct dependence on the density, we find the chiral restoration point to be dangerously close to the saturation value. This would require strong precursors of chiral restoration at normal densities, in sharp contradiction to our knowledge. Thus, the intermediate result of our paper is that straightforward application of the pion nuclear physics to the calculation of the scalar $\bar{q}q$ expectation value in the nuclear matter leads to unphysical results. The problem is solved by self-consistent treatment of the condensate and of hadron parameters.

Indeed, the expectation value of the quark condensate in nuclear matter is calculated by Feynman diagrams technique. The expressions, corresponding to the diagrams, include dependence on a number of in-medium hadron parameters. These are nucleon and pion masses, the coupling constant, the number of quark-antiquark pairs in pion, etc. On the other hand, these in-medium characteristics can be expressed through the averaged values of quark (and gluon) operators in the framework of QCD sum rules [1], or by using other models, e.g. Nambu–Jona-Lasinio–model (NJL). Such models, combined with the idea of scaling, developed by G.E.Brown and M.Rho [14], [15] enable us to express the baryon effective masses m^* , m^*_{Δ} and pion decay constant f^*_{π} , through in-medium value of the quark condensate $(m^*(\kappa), f^*_{\pi}(\kappa))$.

Thus, we solve the following system of equations:

$$\kappa = f_{\kappa}(m^*, ...),$$

$$m^* = f_m(\kappa),$$

with the dots standing for other hadron parameters, depending on κ . As a result, there appears a self-consistent scheme for the calculation of the expectation value of quark condensate κ and effective baryon mass m^* in the medium. The self-consistent calculation leads to a rapid decrease of the effective nucleon mass with density. Thus, there is no pion condensation at least up to the density $\rho = 2.8\rho_0$.

At larger densities $\rho \geq 2.8\rho_0$ the heavier baryons (isobars) can be accumulated in nuclear matter, thus changing the structure of its ground state. Therefore, the first phase transition, which takes place while the density increases is the condensation of heavier baryons in the ground state of nuclear matter. If we neglect the new Fermi sea of isobars, we find that κ approaches zero asymptotically, i.e. at $\rho \to \infty$. Also, there is no pion condensation.

In the self-consistent approach the shape of ρ -dependence of both functions $m^*(\rho)$ and $\kappa(\rho)$ does not change much, while we modify the shape of the dependence $m^*(\kappa)$. Dependence of the values of m^* and κ on the values of parameters describing effective particle-hole interactions and on those of form factors of the pion vertices is also weak.

Scalar quark condensate

Investigation of the scalar condensate can be interesting from several points of view. It may appear to be useful in the attempts to find the bridge between description of strong interactions in hadron and quark-gluon degrees of freedom. Indeed, the condensate is determined through quark degrees of freedom, depending, however on the values of hadron parameters. On the other hand, it describes the properties of the matter as a whole. Being the order parameter of the system, it characterizes the violation of chiral symmetry. Its turning to zero leads to bright consequences for the system as a whole ¹.

Also, we hope that the developing of QCD sum rules project started in [1] will provide the bridge between the two ways of description, based either on hadronic or quark degrees of freedom. By using the QCD sum rules, the particle properties (mass, pole residue, etc.) can be expressed through expectation values of the quark and gluon operators. The scalar condensate $\bar{q}q$ is one of the most important. The expectation values of the vector $\bar{q}\gamma_0q$ and scalar $\bar{q}q$ operators play the role of the vector and scalar boson fields, in terms of the Quantum Hadrodynamics (QHD) approach [16] in the mean field approximation. In this approximation the nuclear matter can be considered as a medium with nonzero expectation value, $\langle M|\bar{q}\gamma_0q|M\rangle\neq 0$, and with a new value of scalar operator $\langle M|\bar{q}q|M\rangle$, which is not equal to the vacuum one.

¹On the other hand, turning of $\kappa(\rho)=<|\bar{q}q|>$ to zero may be not sufficient for the chiral symmetry restoration. It is not excluded that the expectation value $< M|\bar{q}q|M>$ is equal to zero, but simultaneously $< M|\bar{q}q\bar{q}q\bar{q}q|M> \neq 0$, etc. However in many of the models used nowadays, e.g. NJL-model, the value $<|\bar{q}q|>$ may be considered as an order parameter, and the chiral symmetry violation does not take place, although $<|\bar{q}q|>$ turns to zero.

The value of the vector condensate $\langle M|\bar{q}\gamma_0q|M\rangle=3$ $\langle M|\bar{N}\gamma_0N|M\rangle=3\rho$ does not depend on the choice of degrees of freedom. The latter can be quark or hadronic as well. This is due to the vector current conservation. Thus in the latest equality ρ should be treated as the baryon charge density. The density dependence of the scalar quark condensate $\kappa(\rho)=\langle M|\bar{q}q|M\rangle$ is more complicated. It is the subject of the present paper.

Now we run through the main ideas and results of this paper. In the gas approximation [1]

$$\kappa(\rho) = \kappa(0) + \rho < N|\bar{q}q|N>,\tag{1}$$

where $\kappa(0) = <0|\bar{q}q|0> \simeq -0.03 \text{ GeV}^3$ is vacuum expectation, and the number of quarks in a nucleon,

$$< N|\bar{q}q|N> = \frac{2\sigma}{m_u + m_d},$$

is given by the well known πN σ -term: σ =45 MeV, m_u and m_d are the current quark masses.

In a number of papers [1] — [11] attempts were made to go beyond the gas approximation

$$\kappa(\rho) = \kappa(0) + \rho < N|\bar{q}q|N > +S(\rho), \tag{2}$$

with the nonlinear term $S(\rho)$. This contribution comes mainly from the pion exchange because of small pion mass and large expectation value

$$\eta = <\pi |\bar{q}q|\pi> = \frac{2m_{\pi}^2}{m_u + m_d}.$$
(3)

Being a Goldstone meson, the pion describes the collective mode, i.e. the excitation of the large number of $\bar{q}q$ -pairs.

The calculations of $S(\rho)$ in one— and two–loop approximations (i.e. with one— and two–pion exchanges) were done in [1, 9, 11] ². At low density the loop expansion is equivalent to the expansion with respect to the Fermi momentum $p_F \propto \rho^{1/3}$. Each extra loop gives an extra factor $\rho^{1/3}$ (in the case $m_{\pi} \ll p_F$).

Phase transition

At large densities, the different types of the phase transitions can take place in nuclear matter before the quark-gluon plasma formation. There is a number of possibilities:

- i) new types of baryons $(\Lambda, \Sigma, \Delta)$ can appear in the ground state of nuclear matter [17], when the energy of the nucleon on the Fermi surface $(\varepsilon_F = p_F^2/2m)$ becomes larger than the mass splitting $\Delta m = m_B - m$ (B= Λ , Σ , Δ ; $m = m_N$). More precise condition which takes the baryon-hole interaction and the mass renormalization into account will be discussed in Sect. 5 and in a separate paper [18];
- ii) chiral invariance will be restored, when $\kappa(\rho)$ turns to zero;
- iii) the pion condensation [12] can take place.

²Note that erroneous isotopic coefficient was used in [11]. So, the result for φ_1 published in [11] should be multiplied by 3/4.

Let us clarify the latest point. In nuclear medium a pion can be absorbed, producing a free nucleon, or Δ , and a hole. In next step the free baryon can emit a new pion and go back filling up the hole. These transitions can be interpreted as the pion interactions with the particle-hole channels. Thus, instead of the free pion in vacuum one deals with the mixture of the pion and baryon-hole states. These pion—to baryon-hole transitions can be described completely by the polarization operator $\Pi(\omega, k; \rho)$ in the pion propagator D:

$$D = \frac{1}{\omega^2 - m_\pi^2 - k^2 - \Pi(\omega, k; \rho) + i\varepsilon}.$$
 (4)

Here and below $k = |\vec{k}|$. The dispersion equation

$$D^{-1} = \omega^2 - m_{\pi}^2 - k^2 - \Pi(\omega, k; \rho) = 0$$

has several solutions. While the density ρ increases, one of the solutions, $\omega_c(\rho)$, turns to zero. For the first time it happens at a critical density $\rho = \rho_c$ for some concrete value $k = k_c$ of pion momentum. At larger densities $\rho > \rho_c$, the square of ω_c is negative ($\omega_c^2(\rho) < 0$) in some interval of values of k. In this case one has to add the pion-type excitations into the ground state of the nuclear matter. This phenomenon is called the pion condensation [12].

Since there is a large number of pions in the ground state, large contribution to the expectation value $\kappa(\rho)$ appears. Hence, the value of $\kappa(\rho)$ changes near the point $\rho = \rho_c$ significantly. The pion condensation is the main source of nonlinearity in the $\kappa(\rho)$ behaviour.

$<|\bar{q}q|>$ in the presence of "pion condensation"

The aim of this paper is to calculate the quark condensate in the nuclear medium, with account of possible pion condensation.

We will consider the simplest (one-loop) approximation (Fig. 1) but with the exact (renormalized) pion propagator (see Eq. (4)) including geometrical series of baryon-hole insertions.

Of course, this is not the whole set of Feynman graphs, but it describes and includes all the main physical effects we would like to discuss. The short-range interactions will be taken into account in terms of the Theory of the Finite Fermi System (TFFS) [19], by using the effective constants g'_{NN} , $g'_{N\Delta}$, $g'_{\Delta\Delta}$ corresponding to nucleon and Δ -isobar rescatterings. On the other hand, the long-range correlations are described by the exact pion propagator.

Note that in the limit of a small pion-nucleon coupling, our approach reproduces exactly the one-loop result [1], [3] and the most important part of the 2-loop calculations [11].

If the nucleons are treated in nonrelativistic limit, the value of polarization operator, accounting the baryon-hole loop is proportional to the coupling constant g_A^*/f_π^* squared and to the nucleon effective mass m^* :

$$\Pi(\omega, k; \rho) \propto \left(\frac{g_A^*}{f_\pi^*}\right)^2 m^* p_F k^2,$$
 (5)

where m^* , g_A^* and f_π^* are the nucleon mass, axial current and pion coupling in medium, correspondingly. Here and below all effective variables, renormalized in the nuclear medium, are

supplied with an asterisk. The Fermi momentum $p_F \propto \rho^{1/3}$, and for symmetric nuclear matter

$$\rho = \frac{4}{(2\pi)^3} \int^{p_F} d^3k.$$

Factor $p_F m^*$ comes from the integration of the energy denominator, with $\Delta E \sim k^2/2m^*$:

$$\int^{p_F} \frac{d^3k}{\Delta E} \sim m^* p_F.$$

Thus, to calculate the true value of quark condensate $\kappa(\rho)$ one has to know the ρ -dependence of the baryon mass $m^*(\rho)$ and that of the coupling constant g_A^*/f_π^* . The simplest possibilities are to use either the Landau formula [20]

$$\frac{m^*}{m} = \frac{1}{1 + \frac{2mp_F}{\pi^2} f_1},\tag{6}$$

or the Walecka-type model [16], where in nonrelativistic limit

$$m^* = m - c\rho \tag{7}$$

with certain constant coefficients f_1 and c.

Using Eqs. (6) or (7), one obtains the pion propagator pole at $\omega = \omega_c(\rho)$ with $\omega_c^2 \leq 0$ for the densities $\rho \geq \rho_c$. The value of critical density ρ_c turns to be of the order of the saturation one.

Say, the value, obtained in the papers [13], [21], is $\rho_c \sim (1.0 - 1.5)\rho_0$. The appearance of such a pole was interpreted as the signal of "pion condensation" [12].

However, just before the "condensation" (at $\rho < \rho_c$) the nonlinear contribution $S(\rho)$ increases drastically, and the curve $\kappa(\rho)$ crosses the zero line. The reason is trivial. When $\rho \to \rho_c$, the integral for the pion loop (Fig. 1) takes the form

$$S \sim \int \frac{d\omega d^3k}{(\omega^2 - \omega_c^2(\rho, k))^2}$$

(here we keep the singular part of integrand only and take into account the symmetry of pion propagator in respect to the sign of ω). The integral diverges near the condensation point $\omega_c(\rho_c, k) \simeq a \cdot (k - k_c)^2 \to 0$ for $k \to k_c \neq 0$:

$$\int \frac{d\omega k_c^2 d(k - k_c)}{(\omega^2 - a^2 (k - k_c)^4)^2} \to \infty.$$

This means that one faces another phase transition. Namely, the chiral symmetry restoration is reached before the pion condensation. At larger densities the pion does not exist any more as a collective Goldstone degree of freedom, the baryon mass vanishes (if very small contribution of the current quark masses is neglected), and we have to stop our calculations based on the selected set of Feynman diagrams (Fig. 1) with exact pion propagator.

The structure of pion propagator singularities, various branches of solutions of dispersion equation and calculation of the quark condensate $\kappa(\rho)$ under the assumptions described by Eqs. (6) or (7) with the coupling $g_A^*/f_\pi^* = g_A/f_\pi = const$ are described in Sect. 2, 3, 4.

With conventional values of TFFS constants $(f_{\pi}, f_1, g'_{NN},...)$ we obtain $\kappa(\rho) = 0$ at rather small densities $\rho \sim (1.1 \div 1.2)\rho_0$. This does not look to be realistic.

Self-consistent approach

Therefore, we consider another approach, which is a self-consistent one. We obtain the expression for quark condensate κ which depends on nuclear density, on effective mass m^* , on the effective constant f_{π}^* , etc. On the other hand, the effective (renormalized) values of m^* , f_{π}^* ... depend on κ .

Recall, for example, that in the framework of QCD sum rules the baryon mass is determined mainly by the $\bar{q}q$ -expectation value. The relation between the mass and $\kappa(\rho)$ is even more straightforward in the NJL-model. The nucleon (and constituent quark) mass is proportional to κ , and in medium one finds

$$m^*(\rho) = G \cdot \kappa(\rho), \tag{8}$$

where G is the constant for the four-fermion interaction. Thus, in order to perform self-consistent calculations, we have to solve the set of equations

$$\kappa = F_{\kappa}(\rho, m^{*}(\rho), f_{\pi}^{*}(\rho), ...) = \kappa(0) + \rho < N|\bar{q}q|N > +S(\rho),$$

$$\frac{m^{*}(\rho)}{m} = F_{m}(\kappa, \rho),$$

$$\frac{f_{\pi}^{*}(\rho)}{f_{\pi}} = F_{\pi}(\kappa, \rho).$$
(9)

In Sect. 5, we use Eqs. (9), together with a hypothesis about g_A^*/f_π^* behaviour, and calculate the expectation $\kappa(\rho)$. Two types of behaviour of the ratio g_A^*/f_π^* are considered: 1). $g_A^*/f_\pi^* = g_A/f_\pi = const$, which is the latest version of Brown-Rho scaling [15]; and 2). $g_A^* = g_A$; $f_\pi^*/f_\pi = m^*/m$ [14].

Here is our main result. For $g_A^*/f_\pi^* = const$ and

$$\frac{m^*(\rho)}{m} = F_m, \qquad F_m = \frac{\kappa(\rho)}{\kappa(0)},$$

we get rather smooth $\kappa(\rho)$ dependence. The system tries to prevent the chiral symmetry restoration at low densities: the ratio $\kappa(\rho)/\kappa(0) \ge 0.2$ up to $\rho \sim 2.5\rho_0$ ($\kappa(\rho_0)/\kappa(0) = 0.55$).

To study the stability of the results we consider several other possibilities of $m^*(\rho)$ dependence. These are:

$$\frac{m^*(\rho)}{m} = \left(\frac{\kappa(\rho)}{\kappa(0)}\right)^{1/3},$$

and QCD sum rules motivated formula [22]

$$\frac{m^*(\rho)}{m} = \frac{\kappa(\rho)}{\kappa(0)} - \frac{2.4\rho}{\kappa(0)}.$$
(10)

with the second term caused by vector condensate. All the versions with $g_A^*/f_\pi^*=const$ show the same qualitative behaviour. On the contrary, for $g_A^*=const$ and $f_\pi^*/f_\pi=m^*/m$ we reach the critical point $\kappa(\rho)=0$ at a very small value of Fermi momentum $p_F\simeq 200$ MeV ($\rho<\rho_0/2$), since in this case the polarization operator increases while $|\kappa|$ decreases ($\Pi\propto m^*/f_\pi^{*2}\propto 1/\kappa$). The vanishing of the $\bar{q}q$ -expectation value at $\rho\sim\rho_0/2$ does not take place in the Nature. Hence, we have to reject this possibility.

Note that in the present paper we ignore the strange sector, but even in non-strange sector new baryons (Δ -isobars) appear in the ground state of nuclear matter at larger densities. Thus, we cannot continue calculations at $\rho > (2.5 - 3.0)\rho_0$, before the reconstruction of the ground state is carried out.

Since for moderate densities $\rho \sim 2\rho_0$ the effective mass of nucleon m^* becomes comparable with the Fermi momentum p_F , we account for relativistic kinematics of nucleons. In this case we obtained reasonable values of effective nucleon mass $m^*(\rho_0) = 0.6m$ and of the scalar condensate $\kappa(\rho_0) = 0.6\kappa(0)$ for normal nuclear density ρ_0 .

2 The main equations

The lowest order contribution to the quark condensate beyond the gas approximation is provided by the nucleon self-energy graph shown in Fig. 1, with both nucleon and Δ -isobar contributing to the intermediate state. In vacuum all intermediate nucleon momenta $p_2 \geq 0$ are available, but in medium the momenta $p_2 > p_F$ are allowed only, because of Pauli principle (see Fig. 1). Besides, the pion in-medium propagator should be renormalized; this is shown in Figs. 1b,d by fat wavy line. Therefore, we calculate the contribution of the diagrams, shown in Figs. 1b,d subtracting analogous vacuum contributions with bare (vacuum) pion propagator (Figs. 1c,e).

From formal point of view, $\kappa(\rho)$ can be calculated as the derivative of the energy density \mathcal{E} with respect to the current quark mass [2]:

$$\kappa(\rho) = \partial \mathcal{E}/\partial m_q. \tag{11}$$

The pion-induced part comes from the differentiation of the nucleon self-energy Σ_N , which corresponds to the diagram of Fig. 1a

$$S_{\pi}(\rho) = \rho \frac{\partial \Sigma_N}{\partial m_{\pi}^2} \cdot \frac{\partial m_{\pi}^2}{\partial m_q},$$

³As was mentioned in [14], the low density evolution from $g_A(0) = 1.25$ to $g_A(\rho_0) = 1$ has a special explanation.

where the derivative

$$\frac{\partial}{\partial m_{\pi}^{2}} \frac{1}{(\omega^{2} - m_{\pi}^{2} - k^{2} - \Pi)} = \frac{1}{(\omega^{2} - m_{\pi}^{2} - k^{2} - \Pi)^{2}}$$

squares pion propagator, and

$$\frac{\partial m_{\pi}^2}{\partial m_a} = \frac{m_{\pi}^2}{m_a} = \eta/2.$$

Here η is the number of $\bar{q}q$ -pairs in pion (Eq. (3)). We use linear PCAC equation for the pion mass squared m_{π}^2 , obtained by Gell-Mann, Oakes and Renner (GMOR) [23]:

$$m_{\pi}^{2} = -\frac{\langle |\bar{q}q| \rangle (m_{u} + m_{d})}{2f_{\pi}^{2}}.$$
 (12)

In the Feynman graph of Fig. 1, the $\bar{q}q$ operator is shown by the fat black point which i) stands for the pion propagator squared, and ii) multiplies the result by the factor η .

Note that we average the operator $\bar{q}q$ over the pion states but not over intermediate baryon states. Due to the Ward identity, which corresponds here to the baryon number conservation, all the contributions containing $\langle N|\bar{q}q|N\rangle$ for the πN intermediate state are already accounted for by the second term in Eq. (2).

From technical point of view, this is supported by the following argument. For the nucleon in the matter the condensate $< N|\bar{q}q|N>_m$ can be presented as

$$< N|\bar{q}q|N>_m = < N_m|\bar{q}q|N_m> + < N|\bar{q}q|N> \left(-\frac{\partial \Sigma_N}{\partial E}\right).$$

Here $|N\rangle$ is free nucleon state and $|N_m\rangle$ is in-medium nucleon one with energy $E; \Sigma_N$ is the self-energy. Using the multiplicative character of renormalization

$$|N_m>=Z^{1/2}|N>, \qquad \frac{\partial \Sigma_N}{\partial E}=Z-1,$$

we find $\langle N|\bar{q}q|N\rangle_m = \langle N|\bar{q}q|N\rangle$, thus proving our assumption.

For Δ -baryons (Fig. 1), we deal with the contributions proportional to the difference

$$\delta = <\Delta |\bar{q}q|\Delta > - < N|\bar{q}q|N > .$$

Basing on the Additive Quark Model (AQM), we assume that $\delta = 0$. Thus we take into account only the pion contribution to $\kappa(\rho)$.

Certainly, in the strong interactions, there is no reasonable parameter for perturbative series. We consider the first (one-loop) self-energy diagram of Fig. 1 with full (exact) pion propagator instead. In other words, we sum up the selected set of Feynman graphs which are responsible for the lowest singularity in the ρ -dependence of $\kappa(\rho)$. The expression for $S_N(\rho)$, illustrated by Figs. 1b,1c is:

$$S_N(\rho) = -3\eta Sp \int \frac{d^3p}{(2\pi)^3} \frac{d\omega d^3k}{(2\pi)^4i}$$
(13)

$$\left(\Gamma_{\pi NN}^2 D^2(\omega, k) \theta(p_F - p) \frac{\theta(|\vec{p} - \vec{k}| - p_F)}{\varepsilon(p) - \omega - \varepsilon(\vec{p} - \vec{k}) + i\delta} - \Gamma_{\pi NN}^{02} D_0^2(\omega, k) \theta(p_F - p) \frac{1}{\varepsilon(p) - \omega - \varepsilon(\vec{p} - \vec{k}) + i\delta}\right).$$

Here Sp stands for summation over the nucleon spin indices, the factor 3 comes from the summation over isotopic coefficients and the last term is needed to avoid the double counting and subtract the contribution which is already included into $\langle N|\bar{q}q|N\rangle$ in the second term of Eq. (2), which is related to the bare nucleon in a vacuum. Recall that $\rho = 2p_F^3/3\pi^2$. We must add similar contribution of intermediate isobar, illustrated by the diagram of Fig. 1d.

The free pion propagator is

$$D_0 = (\omega^2 - k^2 - m_\pi^2 + i\delta)^{-1}.$$

The πNB vertex with B labeling nucleon or Δ -isobar is

$$\Gamma_{\pi NB} = \Gamma_{\pi NB}^{(0)} \cdot d_B(k) \cdot x_{\pi NB},\tag{14}$$

while

$$\Gamma_{\pi NN}^{(0)} = \frac{g_A}{\sqrt{2} f_\pi} \bar{\psi} \gamma_\mu \gamma_5 \psi k_\mu = \frac{i g_A}{\sqrt{2} f_\pi} \chi^* (\vec{\sigma} \vec{k}) \chi, \tag{15}$$

with $\psi(\chi)$ being the (non)relativistic nucleon four- (two-) spinors. In order to take into account the nonzero baryon sizes, the bare vertex $\Gamma^{(0)}$ is multiplied by the form factor taken in a simple pole form

$$d_B = \frac{1 - m_\pi^2 / \Lambda_B^2}{1 + k^2 / \Lambda_B^2},$$

 Λ_N =0.667 GeV, while Λ_{Δ} =1.0 GeV [24]. The factors $x_{\pi NN}$ and $x_{\pi N\Delta}$ are accounting for the renormalization of the corresponding vertices due to the particle-hole pairs. Explicit expressions for them will be given later on (see Eq. (27)).

The expression, corresponding to the diagram of Fig. 1d with Δ -baryon is analogous to Eq. (13). However, the unrenormalized vertex is now

$$\Gamma_{\pi N \Delta}^{(0)} = f_{\Delta/N} \frac{ig_A}{\sqrt{2} f_\pi} \chi^* (\vec{S}_\alpha^+ \vec{k}) \chi^\alpha. \tag{16}$$

The experiments provide the value of the coupling constant $f_{\Delta/N} \simeq 2$ [24], while AQM calculations give $f_{\Delta/N} \simeq 1.7$.

Certainly, there are no limits for momenta of isobars in the intermediate states. Mass difference $\Delta m = m_{\Delta} - m$ is included into the of Δ -baryon energy $\varepsilon(\vec{p} - \vec{k})$.

We assume that the baryon-medium interactions change the potential energy of any baryon (nucleon or Δ -isobar) by the same value, which does not depend on the baryon momentum p. This is consistent with QHD picture in the mean field approximation, under the assumption that the vector field has the same coupling to nucleon and Δ -baryon. In other words, AQM is assumed to describe the vector field interaction with baryon.

Note that only nonrelativistic approximation for the baryon propagator is used in Sects. 2-5. In Sect. 6, to estimate relativistic effects at large densities (when the Fermi momentum p_F becomes comparable with effective mass m^*) we use traditional perturbative approach, with all particles on the mass shell. Still, we neglect the contribution from badly time-ordered graphs, where the antibaryon-baryon pairs are created.

Therefore, the only relativistic effect (Sect. 6) is a relativistic expression for $\varepsilon(p)$ in the denominator of Eq. (13):

$$\varepsilon_p = \sqrt{(m^{*2} + p^2)}.$$

Now we construct the pion propagator in nuclear matter. According to TFFS, we have to sum up the geometric series of baryon-hole loops shown in Fig. 2a. The contribution of one loop, illustrated by first diagrams in Figs. 2b,c are

$$\Pi_N^{(0)} = Sp \int \frac{d^3p}{(2\pi)^3} \Gamma_{\pi NN}^2 G_N(\vec{p} + \vec{k}) \theta(|\vec{p} + \vec{k}| - p_F) \theta(p_F - p), \tag{17}$$

$$\Pi_{\Delta}^{(0)} = Sp \int \frac{d^3p}{(2\pi)^3} \Gamma_{\pi N\Delta}^2 G_{\Delta}(\vec{p} + \vec{k}) \theta(p_F - p). \tag{18}$$

Here the traces are taken over spin and isospin variables, and G_N , G_{Δ} are nucleon and Δ -isobar propagators.

In the described perturbative series for the baryon-hole loop, we consider both particle-hole excitation and absorption contributions (the first and the second diagrams, correspondingly, in Figs. 2b,c)

Thus,

$$\Pi_N^{(0)} = -4 \left(\frac{g_A^*}{\sqrt{2} f_\pi^*} \right)^2 k^2 \left[\Phi_N(\omega, \vec{k}) + \Phi_N(-\omega, -\vec{k}) \right] d_N^2(k), \tag{19}$$

$$\Pi_{\Delta}^{(0)} = -\frac{16}{9} \left(\frac{g_A^*}{\sqrt{2} f_{\pi}^*} \right)^2 f_{\Delta/N}^2 k^2 \left[\Phi_{\Delta}(\omega, \vec{k}) + \Phi_{\Delta}(-\omega, -\vec{k}) \right] d_{\Delta}^2(k), \tag{20}$$

with Migdal's function

$$\Phi_{\Delta}(\omega, k) = \frac{1}{4\pi^2} \frac{m^{*3}}{k^3} \left[\frac{a^2 - b^2}{2} \ln(\frac{a+b}{a-b}) - ab \right]. \tag{21}$$

Here $a = \omega - k^2/2m^* - \Delta m$, $b = kp_F/m^*$, and $Re(\Delta m) = m_\Delta - m$, $Im(\Delta m) = -\Gamma_\Delta/2$. Γ_Δ is the isobar width.

Integration over the momenta p provides

$$\Phi_N(\omega, k) = \frac{m^*}{k} \frac{1}{4\pi^2} \left(\frac{-\omega m^* + kp_F}{2} + \frac{(kp_F)^2 - (\omega m^* - k^2/2)^2}{2k^2} \ln(\frac{\omega m^* - kp_F - k^2/2}{\omega m^* - kp_F + k^2/2}) \right)$$
(22)

$$-\omega m^* \ln(\frac{\omega m^*}{\omega m^* - k p_F + k^2/2}) \right),$$

at $0 \le k \le 2p_F$, while

$$\Phi_N(\omega, k) = \frac{m^*}{k} \frac{1}{4\pi^2} \left(-\frac{p_F}{k} (\omega m^* - k^2/2) + \frac{(kp_F)^2 - (\omega m^* - k^2/2)^2}{2k^2} \ln(\frac{\omega m^* - kp_F - k^2/2}{\omega m^* + kp_F - k^2/2}) \right)$$
(23)

at $2p_F \leq k \leq \infty$.

Note that Eq. (22) differs from analogous equation of Refs. [13], [24] at $k \leq 2p_F$. The short-range correlations originated from the baryon-hole rescattering are described in terms of TFFS with the help of effective constants g'_{NN} , $g'_{N\Delta}$, $g'_{\Delta\Delta}$, which correspond to N-N, N- Δ and Δ - Δ rescatterings. If it is not specially mentioned, we use $g'_{NN}=1.0$, $g'_{N\Delta}=0.2$, $g'_{\Delta\Delta}=0.8$ [13]. After summation of the geometrical series of baryon-hole loops, we obtain the polarization operator [13], [25]

$$\Pi(\omega, k; \rho) = \Pi_N + \Pi_{\Delta}$$

with

$$\Pi_N = \Pi_N^0 (1 + (\gamma_\Delta - \gamma_{\Delta\Delta}) \frac{\Pi_\Delta^0}{k^2}) / E, \tag{24}$$

$$\Pi_{\Delta} = \Pi_{\Delta}^{0} (1 + (\gamma_{\Delta} - \gamma_{NN}) \frac{\Pi_{N}^{0}}{k^{2}}) / E.$$
(25)

Denominator E has the form

$$E = 1 - \gamma_{NN} \frac{\Pi_N^0}{k^2} - \gamma_{\Delta\Delta} \frac{\Pi_\Delta^0}{k^2} + (\gamma_{NN} \gamma_{\Delta\Delta} - \gamma_\Delta^2) \frac{\Pi_{NN}^0 \Pi_\Delta^0}{k^4}.$$
 (26)

The effective constants γ are related to q', as follows:

$$\gamma_{NN} = C_0 g_{NN}' \left(\frac{\sqrt{2} f_\pi^*}{g_A^*}\right)^2, \gamma_\Delta = \frac{C_0 g_{N\Delta}'}{f_{\Delta/N}} \left(\frac{\sqrt{2} f_\pi^*}{g_A^*}\right)^2, \gamma_{\Delta\Delta} = \frac{C_0 g_{\Delta\Delta}'}{f_{\Delta/N}^2} \left(\frac{\sqrt{2} f_\pi^*}{g_A^*}\right)^2,$$

where C_0 is the normalization factor for the effective particle-hole interaction in the nuclear matter [13]

$$C_0 = \frac{\pi^2}{p_F m^*}.$$

The vertex renormalization factors introduced in Eq. (14) are

$$x_{\pi NN} = (1 + (\gamma_{\Delta} - \gamma_{\Delta\Delta}) \frac{\Pi_{\Delta}^{0}}{k^{2}})/E, \qquad x_{\pi N\Delta} = (1 + (\gamma_{\Delta} - \gamma_{NN}) \frac{\Pi_{N}^{0}}{k^{2}})/E.$$
 (27)

3 Singularities of the pion propagator

We start with the cuts corresponding to singularities of the polarization operator Π . In the complex ω -plane, the nucleon-hole state induces logarithmic cuts on the real axis. As one can see from Eqs. (22-23), Π_N^0 has two cuts at positive ω in the interval $0 \le k \le 2p_F$

$$1) \quad 0 \le \omega \le \frac{kp_F}{m} - \frac{k^2}{2m},\tag{28}$$

2)
$$\frac{kp_F}{m} - \frac{k^2}{2m} \le \omega \le \frac{kp_F}{m} + \frac{k^2}{2m}$$
, (29)

while for large $k \geq 2p_F$ we have one cut only

$$-\frac{kp_F}{m} + \frac{k^2}{2m} \le \omega \le \frac{kp_F}{m} + \frac{k^2}{2m}.\tag{30}$$

The cut caused by the Δ -hole state lays below the real axis (for $Re \ \omega > 0$) at

$$\frac{k^2}{2m} + \Delta m - \frac{kp_F}{m} \le \omega \le \frac{k^2}{2m} + \Delta m + \frac{kp_F}{m},\tag{31}$$

with $Im \ \omega = -\Gamma_{\Delta}/2$.

Besides, there are symmetric cuts at $Re \omega < 0$. The complete structure of the cuts of polarization operator is shown in Fig. 3.

To make the picture more visual we start with fixed $\Gamma_{\Delta}=115$ MeV equal to the width of Δ -isobar in vacuum. On the other hand, the values of ω which are important in our integrals are rather small, and practically there is no phase space for the decay $\Delta \to \pi N$ in the medium. Thus, the Δ -isobar width in the medium $\Gamma_{\Delta}^* \simeq 0$. Therefore, in final computations we put $\Gamma_{\Delta}^* = 0$.

Another set of singularities is provided by the poles of the total pion propagator, i.e. by solutions of the dispersion equation

$$D^{-1} = \omega^2 - k^2 - m_{\pi}^{*2} - \Pi(\omega, k; \rho) = 0.$$
 (32)

 m_{π}^{*} denotes in-medium value of the pion mass, which is equal to

$$m_{\pi}^{*2} = m_{\pi}^2 + \Pi_s$$

with the scalar polarization operator Π_s describing S-wave pion-nucleon rescattering. The polarization operator, provided by Eqs. (24), (25), accounts for the P-waves only. For the analysis, carried out in this Section it is sufficient to use the gas approximation equation

$$\Pi_s = -\rho \frac{\langle N | \bar{q}q | N \rangle (m_u + m_d)}{2f_{\pi}^2}.$$

while in later analysis we use GMOR expression (12) for m_{π}^* and modify the value of f_{π} as well.

Starting analysis of Eq. (32) from small values of densities ($\rho \leq \rho_0$) we find three branches of its solution on the physical sheet.

3.1 The pion branch $\omega_{\pi}(k)$

At $k \to 0$ it starts at $\omega = \pm \sqrt{m_{\pi}^{*2}}$ leaving the physical sheet through the cut of Π_{Δ}^{0} . For example, this takes place at $k \simeq 4m_{\pi}$, when p_{F} =290 MeV. Hence, at large momenta one deals with the Δ -hole excitations instead of pion's ones.

3.2 The sound branch $\omega_s(k)$

It is a slightly changed solution of the equation E=0 (see Eq. (26)). At very small momenta k the admixture of other branches is tiny and the change is negligible. As it should be for the sound wave, $\omega_s = const \cdot k$ for small k. At $k \simeq 0.43m_{\pi}$ (at p_F =290 MeV) this branch leaves for the lower sheet through the second cut of Π_N^0 (see Eq. (29)). At $k > 0.43m_{\pi}$ this solution is on the second unphysical sheet of the complex ω -plane.

3.3 The isobar branch $\omega_{\Delta}(k)$

It is mainly the Δ -hole sound wave. Starting at $Re(\omega_{\Delta}(k=0)) = m_{\Delta} - m$, $Im(\omega_{\Delta}(k=0)) = -\Gamma_{\Delta}/2$, it plunges under the isobar Π_{Δ}^0 cut (at $k=3.8m_{\pi}$, when p_F =290 MeV).

3.4 The "condensate" branch $\omega_c(k)$

This solution comes to the physical sheet through the first cut of Π_N^0 at $p_F > 283$ MeV/c. The "trajectories" of the solution are shown in Fig. 4 for different values of p_F and of Γ_{Δ} . The part which is in the upper half-plane $(Im\ \omega > 0)$ corresponds to the unphysical sheet. For small $p_F \leq 283$ MeV all the trajectory is placed on the unphysical sheet, but at larger p_F it comes down to the physical sheet. Say, for $p_F = 300$ MeV (360 MeV) the solution is on the physical sheet at $k/m_{\pi} = 1.06 \div 2.60$ ($k/m_{\pi} = 0.36 \div 3.91$). This is illustrated by Fig. 4b. In Fig. 4a one can see that the real part of $\omega_c(k)$ decreases with Γ_{Δ} tending to zero, when $\omega_c(k)$ is on the physical sheet. For $\Gamma_{\Delta} = 0$ the solution goes along the negative imaginary axis. Of course, here $\omega_c^2(k) < 0$. Thus this is the singularity responsible for the so-called "pion condensation" [12].

We have several reasons to put the latest words in the quotation marks. To start with, this is not the pion branch (ω_{π}) , but another one. It starts at k=0 at the same point as the pion branch ω_{π} does: $\omega_{\pi}(k=0) = m_{\pi}^*$. However, it goes to the other sheet. Note also, that while $Re \ \omega_c > 0$, the imaginary part of the solution is negative everywhere on the physical sheet. This means that we never face the mode with $Im \ \omega_i > 0$. In other words, there is no "accumulation of pions", contrary to the naive understanding of condensation.

Of course, there are singularities with $Im \ \omega_i > 0$ in the left half-plane of ω . However, these singularities originate from the inverse time-ordered graphs of Fig. 2c. They are caused by the terms $\Phi(-\omega, -k)$ in Eqs. (19), (20). These singularities correspond to "antiparticles" and do not describe solutions which grow with time.

Nevertheless, the fact that even for $\Gamma_{\Delta} = 0$ one obtains a nonzero imaginary part $Im \ \omega_c \neq 0$ and $\omega_c^2 < 0$ signals on certain instability of the solution. When ω_i^2 turns to zero (for any $k = k_c$)

at certain $\rho = \rho_c$, the ground state should be reconstructed. New components, like baryon-hole excitations (with the pion quantum numbers) emerge in the ground state of nuclear matter. Thus, we cannot use the same approach at larger values of $\rho > \rho_c$.

Thus, the appearance of the singularity $\omega_c^2 = 0$ on the physical sheet shows, that phase transition takes place in the nuclear matter.

We have to emphasize that in all calculations here and below we use the Landau effective mass (6) with the coefficient f_1 , which gives $m^*(\rho_0) = 0.8m$; then $g_A^* = 1.0$ and $f_\pi^* = f_\pi = 92$ MeV. The mass splitting $\Delta m = m_\Delta^* - m^* = const$ with $Re\Delta = 292$ MeV. The values of TFFS effective constants are $g'_{NN} = 1.0$, $g'_{N\Delta} = 0.2$, $g'_{\Delta\Delta} = 0.8$. The constant in the $\pi N\Delta$ -vertex (16) is $f_{\Delta/N} = 2$.

The dependence of the concrete values of $\omega_i(k)$ on the values of TFFS constants g'_{NN} , $g'_{N\Delta}$, and $g'_{\Delta\Delta}$, being changed in reasonable limits, is weak. We can say the same about the dependence on the value of the coupling constant $f_{\Delta/N}$. The whole picture is more sensitive to the values of effective mass m^* and to that pion-baryon coupling g_A^*/f_π^* . This will be the subject of the analysis carried out in next Sections.

4 Pion contribution to the quark condensate

In order to carry out integration over ω in the integral in right hand side of Eq. (13), we specify the integration contour in complex plane. The contour should go below the pion propagator singularities in the left half-plane ω and above the singularities in the right one. We have chosen a straight line $Im\ \omega = a \cdot Re\ \omega$ with a slope $a \le 1$. Since the Cauchy integral is convergent, the result of integration does not depend on the slope value a, that is proved by our computations.

The results of calculation of the function $S(\rho)$, defined by Eqs. (2), (13) are shown in Fig. 5. For the sake of convenience, we display the ratio

$$\frac{\kappa(\rho)}{|\kappa(0)|} = -1 + \rho \frac{\langle N|\bar{q}q|N\rangle}{|\kappa(0)|} + \frac{S(\rho)}{|\kappa(0)|}.$$
(2.1)

The most interesting events take place at p_F between 270 MeV and 320 MeV. The large change of the values of $S(\rho)$ is due to the "pion condensation" singularity ω_c , coming to the physical sheet very close to the integration contour at $p_F = 283$ MeV.

Fig. 5a illustrates the weak dependence of the behaviour of the function $S(\rho)$ on the values of TFFS parameters and on that of $f_{\Delta/N}$.

The value of the width of Δ -isobar is much more important. At smaller Γ_{Δ} the resonance-like structure becomes more pronounced (see Fig. 5b). The peak becomes higher and more narrow. At $\Gamma_{\Delta} \to 0$ the poles at $\omega = \omega_c(k)$ pinch the contour at $\omega_c(k_c) = 0$, $k_c \neq 0$ leading to the infinite value of $S(\rho)$, when the "pion condensate" singularity emerges for the first time on the physical sheet at $\omega_c = 0$. Recall that namely zero value of Γ_{Δ} is expected in nuclear medium for a small ω .

However, as is was discussed in the Introduction, before the pole at $\omega = \omega_c$ (at $\rho = \rho_c$)

reaches the physical sheet, $S(\rho)$ becomes so large that it cancels the negative vacuum expectation value $\kappa(0) \simeq -0.03 \text{ GeV}^3$, and the whole scalar quark condensate turns to zero. The vanishing of the scalar quark condensate indicates the chiral invariance restoration, and after that one has to deal with quite another system, i.e. with another phase of the nuclear matter.

The prediction of chiral phase transition at rather low values of ρ (close to normal nuclear density ρ_0) looks too strong. On the other hand, the results are stable enough and do not change too much under the variation of TFFS parameters and that of $f_{\Delta/N}$. These statements are true for both types of behaviour of nucleon effective masses. However, the dependence on the numerical values of the coefficient which enter Eqs. (6), (7) is strong. The coefficient can be fixed by the choice of the value of $m^*(\rho_0)$. The results for $m^*(\rho_0) = 0.8m$ and for $m^*(\rho_0) = 0.7m$ are compared in Fig. 5c. In the latter case, for the smaller effective mass, the phase transition takes place at $p_F \simeq 320$ MeV, i.e. at larger values of density.

5 Self-consistent approach

5.1 Assumptions on the density behaviour of hadron parameters

As we showed above, the phase transition (either "pion condensation" or chiral symmetry restoration) density value depends strongly on the value of baryon effective mass m^* . On the other hand, in the framework of commonly used models the hadron mass depends mainly on the scalar quark condensate $\kappa(\rho)$. This problem should be solved self-consistently.

Of course, it would be nice to calculate all the masses $(m^*, m_{\Delta}^*, m_{\pi}^*)$ and constants $(g_A^*, f_{\pi}^*,...)$ with the help of QCD sum rules, substituting them in the next step into our expression for $\kappa(\rho)$, solving the equation

$$\kappa = \kappa(\rho, m^*(\rho, \kappa), f_{\pi}^*(\rho, \kappa), \dots) \tag{33}$$

in the final step. Unfortunately, it is not so easy. One of the main obstacles is that the masses and hadron constants depend not on the value of the scalar quark condensate only but on the in-medium expectation values of other operators (usually, more complicated ones) as well.

Therefore, we use simplified scenario of the κ dependence of the mass m^* and of the other parameters involved.

Fortunately, there are model-independent equations. The GMOR relation can be generalized to the case of finite density due to PCAC:

$$m_{\pi}^{*2} = -\frac{\kappa(\rho)}{2f_{\pi}^{*2}}(m_u + m_d). \tag{34}$$

Also, due to chirality, the number of quark-antiquark pairs inside pion is

$$\eta^* = \frac{2m_\pi^{*2}}{(m_u + m_d)}. (35)$$

Now we come to model-dependent relations. Denote the ratios

$$\alpha(\rho) = \frac{m^*}{m}, \quad \beta(\rho) = \frac{f_{\pi}}{f_{\pi}^*}.$$
 (36)

In the NJL-model [14],

$$\alpha(\rho) = \frac{\kappa(\rho)}{\kappa(0)}.\tag{37}$$

In order to check the stability of our result, we perform the calculations using the two more types of κ -dependence of α :

$$\alpha(\rho) = \left(\frac{\kappa(\rho)}{\kappa(0)}\right)^{1/3}.$$
 (38)

This latter expression can be justified by the dimensional counting, if there is only one dimensional parameter. Unfortunately, in our case, this argument does not work, since there are at least two external dimensional parameters ρ and Λ_{QCD} ,

Another expression for $\alpha(\rho)$ is motivated by the QCD sum rules analysis [22]:

$$\alpha(\rho) = \frac{\kappa(\rho)}{\kappa(0)} - \frac{2.4\rho}{\kappa(0)} \tag{39}$$

with the last term in the right hand side caused by the vector condensate.

Now we discuss the in-medium behaviour of pion decay constant f_{π}^* , which is proportional to the pion radius inverted, i.e. $f_{\pi} \propto \sqrt{N_c}/r_{\pi}$ [26]. In the NJL-model near the phase transition point $(\kappa \to 0)$, the pion radius increases unlimitedly, and $f_{\pi} \to 0$ when $\kappa = \langle |\bar{q}q| \rangle \to 0$. Thus, it looks natural to assume that

$$\frac{f_{\pi}^*}{f_{\pi}} = \frac{m^*}{m}.$$

Brown and Rho [14] made even stronger hypothesis assuming that all the parameters of the same dimension are proportional to each other

$$\frac{m^*}{m} = \frac{m_{\Delta}^*}{m_{\Delta}} = \frac{f_{\pi}^*}{f_{\pi}} \dots = \alpha(\rho), \text{ i.e. } \beta = \frac{1}{\alpha}, \tag{40}$$

while the dimensionless parameters do not change in nuclear medium; in particular, (see footnote 3)

$$g_A^* = g_A = const.$$

The second, alternative hypothesis is based on the idea of confinement. If the deconfinement phase transition does not take place simultaneously with the chiral invariance restoration, the pion radius should be limited and f_{π}^* has a nonzero value when we approach the chiral transition point. Therefore, we consider below another limiting possibility:

$$f_{\pi}^* = f_{\pi}$$
, i.e. $\beta = 1$. (41)

In the present calculations we have fixed the value of the axial coupling constant, $g_A^* = 1$. The most important parameter in our calculation is the ratio g_A^*/f_π^* (see Eq. (5), (19), (20)). Thus, just as in the latest version of Brown-Rho scaling [15], $g_A^*/f_\pi^* = const$, i.e. does not depend on ρ .

Note that both hypotheses, described by Eqs. (40), (41) are consistent with the QCD sum rules for pion [27], which can be generalized for the case of finite density in a straightforward way (the proof will be published elsewhere):

$$\frac{\pi}{2} \left(\frac{f_{\pi}^* m_{\pi}^{*2}}{m_u + m_d} \right)^2 = \frac{3W_0^{*4}}{32\pi} \left(\frac{\alpha_s(W_0^{*2})}{\alpha_s(\mu)} \right)^{8/b} + \frac{\pi}{16} < \frac{\alpha_s}{\pi} G_{\mu\nu}^2 > . \tag{42}$$

Here W_0^* is the continuous threshold value, i.e. the minimal energy of the multihadronic states with pion quantum numbers; α_s is the QCD coupling and $G_{\mu\nu}^2$ is the gluon field squared.

Neglecting the last (numerically small) term and anomalous dimension (i.e. putting $\alpha_s(W_0^2) = \alpha_s(\mu)$), one can satisfy Eq. (42) in two ways: (i) $f_{\pi}^* = f_{\pi} = const$ and the threshold position $W_0^{*2} \propto m_{\pi}^{*2}$, or (ii) the fixed threshold $W_0^* = W_0 = const \sim 1$ GeV and Eq. (40) is consistent with for $f_{\pi}^* \propto \kappa(\rho)$

We must also make assumptions on in-medium value of the Δ -isobar mass. If Eq. (40) is true, the Δ -isobar–nucleon mass splitting satisfies the relation

$$\frac{(m_{\Delta}^* - m^*)}{(m_{\Delta} - m)} = \frac{\Delta m^*}{\Delta m} = \alpha(\rho) = \frac{1}{\beta}.$$

However, if $\beta = 1$ (Eq. (41)) we come to $\Delta m^* = \Delta m$.

The experimental situation with Δ -isobar mass in nuclear matter is not quite clear at the moment. On the one hand, the total photon-nucleus cross section indicates that the mass m_{Δ}^* does not decrease in the medium [28], while the nucleon mass $m^*(\rho)$ diminishes with ρ . This means that the splitting Δm^* increases $(\Delta m^* > \Delta m)$, opposite to the $\rho - \pi$ mass splitting. This fact (if it does take place) looks strange, since the two kinds of splitting are caused by the same colour magnetic (spin-spin) quark-quark interaction. On the other hand, the experimental data for total pion-nucleus cross sections [29] are consistent with the mass m_{Δ}^* decreasing in the matter. As to calculations, the description within the Skirmion model [30] predicts that m_{Δ}^* decreases in nuclear matter and $\Delta m^* < \Delta m$. Equation $\Delta m^* = \Delta m$ is also true in Walecka model, if AQM prediction for the scalar field-baryon coupling $g_{sNN} = g_{s\Delta\Delta}$ is assumed.

Thus we expect that the phenomenological parametrization,

$$\frac{\Delta m^*}{\Delta m} = \frac{1}{\beta(\rho)},$$

i.e. $\Delta m^* = \Delta m$ when $\beta = 1$ does not look too unlike.

5.2 A rejected scenario

Here we try the scaling, provided by Eq. (40), with $\alpha(\rho)$ given by (37) and $\beta = 1/\alpha$. We find the phase transition to take place at the densities, about 2.5 times smaller than the normal one, ($p_F \simeq 200 \text{ MeV}$).

The technical explanation is simple. Polarization operator given by Eqs. (5,19,20,24-26), which is responsible for the "pion condensation" singularity $\omega_c(k)$, behaves as

$$\Pi \propto \frac{m^*}{f_{\pi}^{*2}} \propto \frac{1}{\kappa(\rho)} \propto \frac{1}{\alpha(\rho)}.$$

While the density ρ increases, the value of $|\kappa(\rho)|$ and that of $\alpha(\rho)$ become smaller. Polarization operator increases and the "pion condensate" singularity ω_c approaches the physical sheet at smaller p_F . The nonlinear pion contribution $S(\rho)$ becomes very large and the whole value $\kappa(\rho)$ tends to zero (dashed curves in Fig. 7). Also, since $\Pi \propto 1/\alpha(\rho) \to \infty$ when the value of $\kappa(\rho)$ turns to zero, we lose the solution of equation (33) for $\kappa(\rho)$ (see Appendix for details), which from now on becomes the complex one.

Since that, one has to deal with another phase of the matter, with much smaller particle masses. The whole picture contradicts sharply to our knowledge about nuclei and nuclear matter. Thus, we reject this scenario.

5.3 An accepted scenario

For $\beta = 1$ (Eq. (41)) the situation looks much better. Up to $\rho \simeq 2.5\rho_0$, we deal with a self-consistent solution of the system (9). The value of quark condensate tends to zero, when that of the density ρ increases, and we never reach either the chiral symmetry restoration or "pion condensation".

Self-consistent set of Eqs. (9), is solved numerically using the standard iteration procedure. Technically this means, that calculation of $\kappa(\rho)$ with vacuum parameters is followed by calculation of $\alpha(\rho)$. In the next step we obtain in-medium values of all the other parameters by using Eq. (40). This enables us to obtain Π_N and Π_Δ provided by Eqs. (24)-(27). In the last of the cycle substitution of these operators into Eq. (13) for further integration provides a new value of $\kappa(\rho)$. Thus we come to a new cycle.

The validity of our calculations for the larger values of ρ is limited by another phase transition. At some value of Fermi momentum $(p_{F\Delta} \propto \rho_{\Delta}^{1/3})$, the total energy of a nucleon on Fermi surface becomes larger than the energy of the Δ -isobar at rest, i.e. $E_{\Delta}(0) \leq E_{N}(p_{F})$. Thus, the isobars starts to be accumulated by the ground state of nuclear matter. This effect, as well as possible appearance of other types of baryons, can be taken into account in our scheme. Thus our calculations are reliable below p_{F} , corresponding to this phase transition and mark the corresponding points by the black circles on the curves shown in Figs. 6, 7.

From the technical point of view, the effect of instability with respect to the Δ -isobar accumulation in the ground state reveals itself in the fact that the branching points (left edge of the right Δ -hole cut (with $Im \ \omega < 0$) and right edge of the left Δ -hole cut (see Fig. 3))

cross the vertical axis $Im \omega=0$. And two Δ -hole cuts start to deform, i.e. to cross or to pinch (for $\Gamma_{\Delta}=0$) the integration contour in the ω -plane (Eq. (13)).

The possibility for a other, but nucleons, types of baryons to be contained in the nuclearmatter ground state was discussed in [17]. The case of Δ -isobar in the presence of a pion condensate was considered in [31], [32]; the problem without the π -condensation was studied in terms of Walecka model in [33], [34].

The results plotted in Fig. 6a (in terms of $\kappa(\rho)$) and Fig. 6b (in terms of $m^*(\rho)$) do not change too much under reasonable variations of the TFFS couplings. Instead of $g'_{NN}=1.0$ in the master version (solid curve), in Fig. 6 we put $g'_{NN}=0.7$ (dot-dashed curve); for dotted curve $g'_{\Delta\Delta}=1.2$ instead of 0.8; for dashed curve $f_{\Delta/N}=1.7$ instead of 2.0. In all calculations in this Section we have used $\Gamma_{\Delta}=0$.

The lower solid line in Fig. 6b (and Fig. 7b) is drawn for the limit values of m^*/m at every value p_F . If the ratio m^*/m is smaller than the limit value, the ground state of nuclear matter contains isobars. The equation for this line is determined by the condition that the isobar logarithmic cut (Eq. (31)) of the polarization operator Π^0_Δ (Eq. (20)) touches the vertical axis $Im \ \omega = 0$ see (Fig. 3).

In Fig. 7 we demonstrate the dependence of the value of the scalar condensate on the type of the scaling function $\alpha(\rho)$. Solid curve corresponds to the master version, with $\alpha(\rho)$ given by Eq. (37) and $\beta = 1$. Two other parametrizations, provided by Eqs. (38), (39) shown by dotted and dot-dashed curves. The results, corresponding to the law, described by Eq. (38), differ quantitatively from the two others. However, as we said earlier, the latter are better based.

6 Account of relativistic kinematics

At moderate densities of about twice the normal value, the value of effective mass m^* becomes comparable with that of Fermi momentum. Thus, one cannot neglect the relativistic effects any more. We take into account relativistic kinematics by using relativistic expression for the energies $\varepsilon_k = \sqrt{(m^{*2} + k^2)}$ in all the formulae. However, we still omit the baryon-antibaryon pair contributions.

In terms of traditional perturbative theory, Eqs. (21)-(23) should be replaced now by:

$$\Phi(\omega, k) = \Phi_N^{(1)}(\omega, k)\theta(p_F - k) + \Phi_N^{(2)}(\omega, k)\theta(2p_F - k)\theta(k - p_F) + \Phi_N^{(3)}(\omega, k)\theta(k - 2p_F); \quad (43)$$

$$\Phi_N^{(1)}(\omega, k) = \int_{p_F - k}^{p_F} dp A(\omega, k), \quad \Phi_N^{(2)}(\omega, k) = \int_{k - p_F}^{p_F} dp A(\omega, k) + \int_0^{k - p_F} dp B(\omega, k),$$

$$\Phi_N^{(3)}(\omega, k) = \int_0^{p_F} dp B(\omega, k),$$

where

$$A(\omega, k) = \frac{p}{4\pi^2} \frac{m^*}{k} \frac{m^*}{\sqrt{(p^2 + m^{*2})}} \ln\left(\frac{\sqrt{(p_F^2 + m^{*2})} - \omega - \sqrt{(p^2 + m^{*2})}}{\sqrt{((p + k)^2 + m^{*2})} - \omega - \sqrt{(p^2 + m^{*2})}}\right), \tag{44}$$

$$B(\omega, k) = \frac{p}{4\pi^2} \frac{m^*}{k} \frac{m^*}{\sqrt{(p^2 + m^{*2})}} \ln \left(\frac{\sqrt{((p-k)^2 + m^{*2})} - \omega - \sqrt{(p^2 + m^{*2})}}{\sqrt{((p+k)^2 + m^{*2})} - \omega - \sqrt{(p^2 + m^{*2})}} \right); \tag{45}$$

$$\Phi_{\Delta}(\omega, k) = \int_{0}^{p_{F}} \frac{p}{4\pi^{2}} \frac{m^{*}}{k} \frac{(m^{*} + m_{\Delta}^{*})}{2\sqrt{(p^{2} + m^{*2})}} \ln \left(\frac{\sqrt{((p-k)^{2} + m_{\Delta}^{*2})} - \omega - \sqrt{(p^{2} + m^{*2})}}{\sqrt{((p+k)^{2} + m_{\Delta}^{*2})} - \omega - \sqrt{(p^{2} + m^{*2})}} \right).$$
(46)

By using these relativistic expression, we can extend the self-consistent calculation up to $\rho \simeq 2.8\rho_0$. The limit is still determined by transition to the isobar accumulation phase. The results of calculation of the scalar condensate for the three considered possibilities of dependence of the effective mass on κ are presented in Fig. 8. In the QCD sum rules motivated parametrization, described by Eq. (39) with $\beta = 1$, we find $m^*/m = 0.67$, at normal nuclear density $\rho = \rho_0$. And we have $m^*/m = 0.6$ in parametrization (37) with $\beta = 1$. The value is in good agreement with the one, obtained recently in framework of QHD [35].

7 Summary

Since the gas approximation equation for the quark condensate $\kappa(\rho)$ was presented in [1], the nonlinear contribution $S(\rho)$ was considered in a number of papers. The analysis of M.Ericson et al. [7], [8] was based on the general properties of the πN scattering amplitude and its generalization for the case of nuclear medium. As usually, some uncertainties come from the fact that one deals with the off-mass-shell amplitude. Thus, certain assumptions about the NN-interaction and on ρ -dependence of the effective pion mass m_{π}^* in medium are needed.

Another group of papers [3], [4], [8] was based on NJL-model. However, in this case they discussed not the nuclear (build up of the hadrons) medium but the quark one (the quark plasma). In such approach the pion constant f_{π}^* tends to zero, while the mass $m_{\pi}^* \to \infty$ near the point of chiral invariance restoration. As we discuss in Sect. 5, this looks unlikely for the real nuclear matter.

Our approach is based on using the exact pion propagator, renormalized in nuclear medium by the insertions of the nucleon-hole and Δ -hole loops. The short-range correlations are accounted for by methods of TFFS. The lowest laying singularity in ρ corresponding to the so-called "pion condensation" is included. We carried out self-consistent calculations with the quark condensate $\kappa(\rho)$ depending on the effective mass $m^*(\rho)$, while the mass $m^*(\rho)$ itself is determined by (or strongly depends on) $\kappa(\rho)$. Nonlinear ρ -dependence of κ is obtained by calculation of the diagram, shown in the graph of Fig. 1. Calculations include the in-medium values of nucleon, isobar and pions masses and other parameters $(f_{\pi}^*, g_A^*, g'..)$. On the other hand, QCD sum rules and NJL-model give the relations between masses and quark condensates which can be used to determine the in-medium masses and parameters, if $\kappa(\rho)$ is known. This enabled us to solve the set of equations (9).

It should be emphasized that, since the dependence of $m^*(\rho, \kappa(\rho))$ on $\kappa(\rho)$ was treated self-consistently, the "pion condensation" singularity was pushed out from the physical sheet. The only effect which can limit the validity of our calculations at large densities is the accumulation of isobars in the ground state of nuclear matter at $\rho \simeq 2.8\rho_0$. In the general case one should include the possible accumulation of hyperons. To understand, which of the condensates appears earlier, one should have better knowledge of hyperon interactions with matter. Analysis of the problem was started by Pandharipande [17]. This goes beyond the scope of our paper.

At small densities the nonlinear term $S(\rho)$ diminishes the absolute value of $\kappa(\rho)$ in comparison with the gas approximation (the tendency which was already noted in [11] for very low ρ). In our self-consistent approach such behaviour continues up to $\rho \simeq 2.0\rho_0$.

Taking relativistic kinematics into account, we have calculated the expectation values of scalar quark condensate in the symmetric nuclear matter up to $\rho \simeq 2.8\rho_0$, where κ reaches the value $\kappa(2.8\rho_0) \simeq 0.1\kappa(0)$. At normal nuclear density $\rho = \rho_0 = 0.17$ fm⁻³, we obtain $\kappa(\rho_0) \simeq 0.6\kappa(0)$ and the effective nucleon mass $m^*(\rho_0) \simeq 0.6m$. The latter result is very close to the value used nowadays in QHD [35] to describe the properties of nuclei.

Acknowledgments

We are grateful to A.A.Anselm, I.B.Khriplovich, G.Z.Obrant and M.Rho for useful discussions. This work was supported by the Russian Fund of Fundamental Research, Grant No. 96-15-96764

7.1 Appendix

To clarify what happens in the case of scaling, described by Eq. (40) we omit dependence of polarization operator on pion momentum k using the mean value of polarization operator $\overline{\Pi}$ instead. The quark condensate $|\kappa(\rho)|$ obtained in such a way is plotted in Fig. 9 as a function of $\overline{\Pi}$ for two values of density. One can see the dependence to be a monotonous one. The curves A1 and B1, calculated for $\rho = \rho_A$ and for $\rho = \rho_B > \rho_A$ are shown as A1 and B1 in Fig. 9. At some value $\overline{\Pi} = \Pi_c$, when the "pion condensation" singularity ω_c comes the physical sheet, the function $\kappa(\rho, \Pi_c) \to \infty$. While both second and third terms of Eq. (2) increase with ρ (for $S(\rho)$ an extra multiplicative factor ρ comes from the integral over the nucleon momenta), the function $\kappa(\rho, \overline{\Pi})$ becomes steeper for a larger density. To find self-consistent solution in this simplified approximation, we have to solve the set of equations

$$\kappa = \kappa(\rho, \overline{\Pi}),\tag{47}$$

$$\overline{\Pi} = \Pi(\rho, \kappa). \tag{48}$$

We show the function $\overline{\Pi}(\rho, \kappa)$ by curves A2 and B2 in the same figure. The crossing points of A1 and A2 (of B1 and B2) provide the solution.

It was shown in Sect. 1.2 that the polarization operator can be approximated as $\overline{\Pi}(\kappa, \rho) \sim \rho^{1/3}/\kappa$. So $\overline{\Pi} \to \infty$ at $\kappa \to 0$ and the mean value of $\overline{\Pi}$ increases with ρ .

At low densities, there are two solutions: point 1 and point 2, where the curves A1 and A2 cross. For $\rho \to 0$ the first one (κ_1 in point 1) matches smoothly with the solution of NJL gap equation in vacuum: $\kappa_1 \to \kappa(0)$ when $\rho \to 0$. When the density ρ increases the solutions 1 and 2 draw nearer, merge with each other (at some $\rho = \rho_c$) and go out into the complex plane. In this way we lose the real solution at $\rho > \rho_c$.

Assuming that the baryon radius (i.e. parameter Λ in the form factors d_N , d_Δ (see Eq. (14)) follows the same scaling law ($\Lambda^*/\Lambda = f_\pi^*/f_\pi = ...$), one obtains more complicated function $\overline{\Pi}(\kappa)$ shown in Fig. 9b. Now for a very small κ the form factors d_N, d_Δ cut off the integral in the right hand side of Eq. (13) at $k \sim \Lambda << p_F$. Therefore, the effective polarization operator $\overline{\Pi}(\kappa)$ reaches its maximum value and falls down when $\kappa \to 0$, proving us with the third solution with a very small quark condensate $|\kappa| = \kappa_3$ and thus with very small values of hadron masses. This solution does not disappear even at very large densities ρ . On the other hand, for the third solution somewhere at $\alpha = \kappa_3/\kappa(0) \le 0.25$ the pion mass

$$m_{\pi}^{*2} = m_{\pi}^2 \frac{\kappa(0)}{\kappa_3} \propto \frac{1}{\kappa_3}$$

becomes larger the nucleon mass

$$m^* = m \frac{\kappa_3}{|\kappa(0)|} \propto \kappa_3,$$

and we cannot any more apply our approach, based on the summation of a selected set of Feynman diagrams corresponding to the lightest pion degrees of freedom.

In any case, at $\rho \geq \rho_c$ we lose the primary real solution 1 and face a first order phase transition (mass of a hadron has a discontinuity) which looks rather strange.

References

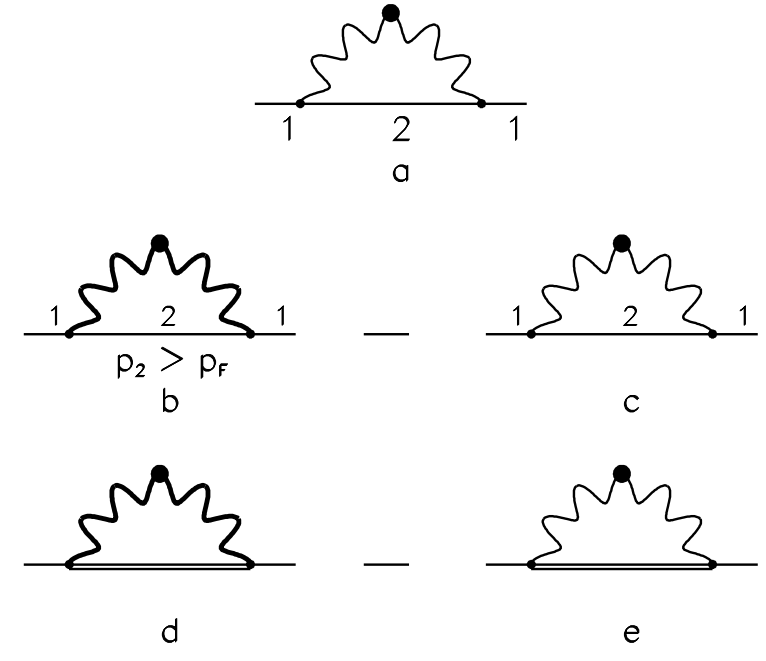
- [1] E.G.Drukarev and E.M.Levin: JETP Lett. 48 (1988) 338
- [2] T.D.Cohen, R.J.Furnstahl, and D.K.Griegel: Phys.Rev. C45 (1992) 1881
- [3] M.Lutz, S.Klimt, and W.Weise: Nucl. Phys. **A542** (1992) 521
- [4] L.S.Celenza, A.Pantziris, and C.M.Shakin: Phys.Rev. C45 (1992) 2015; C46 (1992) 571
- [5] L.S.Celenza, C.M.Shakin, W.D.Sun, and X.Zhu: Phys.Rev. C48 (1993) 159
- [6] M.Jaminon and G.Ripka: Nucl. Phys. **A564** (1993) 505
- [7] M.Ericson: Phys.Lett. **B301** (1993) 11
- [8] G.Chanfray and M.Ericson: Nucl. Phys. **A556** (1993) 427

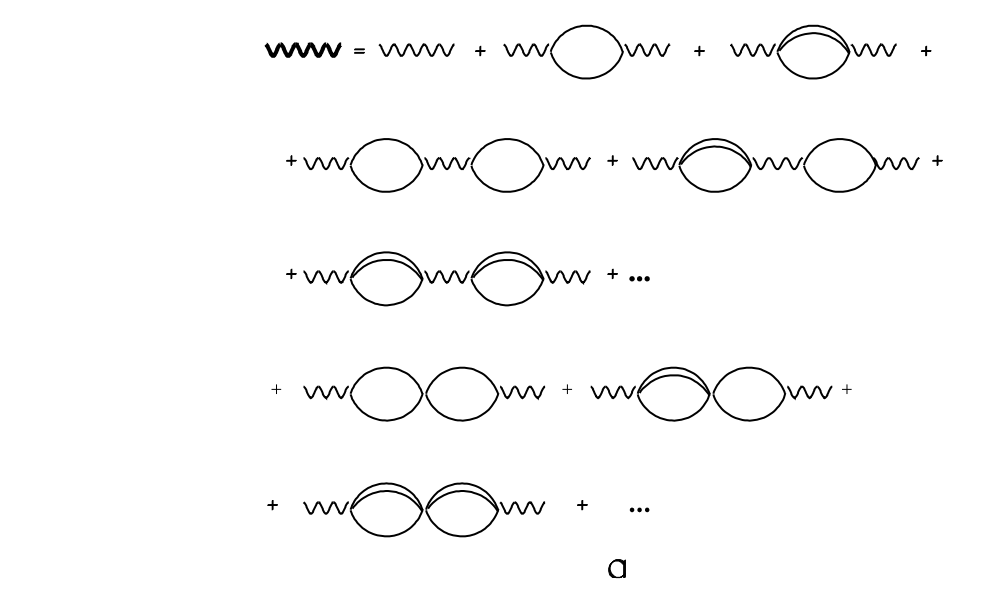
- [9] E.G.Drukarev and M.G.Ryskin: Nucl. Phys. **A578** (1994) 333
- [10] M.C.Birse: J.Phys. **G 20** (1994) 1537
- [11] E.G.Drukarev, M.G.Ryskin, and V.A.Sadovnikova: Z.Phys. **A353** (1996) 455
- [12] A.B.Migdal: JETP **34** (1972) 1184
- [13] A.B.Migdal, D.N.Voskresensky, E.E.Saperstein, M.A.Troitsky: "Pion degrees of freedom in nuclear medium"." Nauka", Moscow, 1991.
- [14] G.E.Brown and M.Rho: Phys.Rev.Lett. **66** (1991) 2720
- [15] G.E.Brown and M.Rho: Phys.Rep. **269** (1996) 333
- [16] J.D.Walecka: Ann. of Phys. 83 (1974) 1491
- [17] V.R.Pandharipande: Nucl.Phys. **A178** (1971) 123
- [18] E.G.Drukarev, M.G.Ryskin, and V.A.Sadovnikova: in preparation
- [19] A.B.Migdal: "Theory of Finite Fermi Sistems and Applications to Atomic Nuclei", New-York, 1967
- [20] L.D.Landau: JETP **30** (1956) 1058
- [21] T.Shamsunnahar, S.Saha, K.Kabir, L.M.Nath: J.Phys. **G17** (1991) 887
- [22] E.G.Drukarev and E.M.Levin: Prog. Part. Nucl. Phys. 27 (1991) 77
- [23] M.Gell-Mann, R.Oakes, and B.Renner: Phys.Rev. 175 (1968) 2195
- [24] T.Ericson, W.Weise: "Pions and nuclei". Clarendon Press, 1988
- [25] W.H.Dichkoff, A.Faessler, J.Meyr-ter-Vehn, and H.Muther: Phys.Rev. C23 (1981) 1154
- [26] R.D.Carlitz, D.B.Creamer: Ann of Phys. 118 (1979) 429; C.E.I.Carneiro, N.A.McDougal: Nucl. Phys. B245 (1984) 293
- [27] M.Shifman, A.Vainshtein, and V.Zakharov: Nucl. Phys. B147 (1979) 385
- [28] N.Bianchi, V.Muccifora, E.De Santis et.al.: Phys.Rev. C54 (1996) 1688
- [29] A.S.Carrol, I-H.Chiang, C.B.Dover et.al.: Phys.Rev. C14 (1976) 635
- [30] A.M.Rakhimov, F.C.Khanna, U.T.Yakhshev, M.M.Masakhanov: nucl-th/9806062
- [31] M.A.Troitsky and N.I.Checunaev: Sov.J.Nucl.Phys. 29 (1979) 220
- [32] B.L.Birbrair and A.B.Gridnev: Preprint LNPI 1441 (1988)
- [33] J.Boguta: Phys.Lett. **B109** (1982) 251
- [34] D.S.Kosov, C.Fuchs, B.V.Martemyanov, and A.Faessler: Phys.Lett **B** to be published
- [35] B.J.Furnstahl, B.D.Serot, and H.B.Tang: Nucl. Phys. A598 (1996) 539

Figure captions

- Fig. 1. a) Diagrammatic representation of the interaction of the operator $\bar{q}q$ (fat point) with the pion field. Straight line denotes the nucleon; the wavy line stands for the pion. b,c) Diagrammatic expression for Eq. (13) with nucleon in the intermediate state. Thick wavy line denotes the pion propagator renormalized due to baryon-hole excitations in the framework of TFFS. d,e) Diagrammatic expression for Eq. (13) with Δ -isobar (double solid line) in the intermediate state.
- Fig. 2. a) Full pion propagator in the medium (thick wavy line) equal to the sum of the geometrical series of the nucleon-hole and isobar-hole excitations. b) Polarization operator of the pion, Π_N^0 , consists of two terms corresponding to excitation and absorption of the nucleon-hole pair. c) Pion polarization operator, Π_{Δ}^0 , consists of two terms corresponding to excitation and absorption of the isobar-hole pair. Thin wavy line denotes a free pion, solid line with left arrow is a hole, solid line with right arrow denotes a nucleon, double line is Δ -isobar.
- Fig. 3. Positions of singularities of the polarization operator Π in the ω -plane (represented at $p_F = p_{F0}$ and $k = m_{\pi}$). On the right half-plane ω/m_{π} , in the interval $\omega/m_{\pi} = 0.0 \div 0.26$, there is the first logarithmic cut of the Π_N^0 -function, see Eq. (28). Moving after thin arrow from the physical sheet across the first cut, we continue the movement on the upper logarithmic sheet (thick arrow). In the interval $\omega/m_{\pi} = 0.26 \div 0.45$ there is the second logarithmic cut of Π_N^0 , see Eq. (29). In this case, following the thin arrow across the second cut we come to the lower logarithmic sheet (dashed arrow). Logarithmic cut of the Π_{Δ}^0 -function is located at $Re \ \omega/m_{\pi} = 1.82 \div 2.54$ and $Im \ \omega = -\Gamma_{\Delta}/2 = -0.115/2$ GeV. Since Π_N^0 and Π_{Δ}^0 are symmetrical in $\omega \leftrightarrow -\omega$ permutation (Eqs. (19), (20)), there are symmetrical cuts on the left half-plane ω/m_{π} .
- Fig. 4. The condensate branch $\omega_c(k)/m_\pi$. a) $\omega_c(k)$ is presented at $p_F = p_{F0}$ for isobar widths values $\Gamma_{\Delta} = 0.001$, 0.01, 0.05, 0.115 GeV (curves 1,2,3,4, correspondingly). Solid lines are disposed on the upper (unphysical) sheet of the first logarithmic Π_N^0 cut. Continuation of this branch to the physical sheet is displayed by dashed curves. All curves begin at k = 0 in the point $\omega = m_\pi^* = 0.80 m_\pi$ (Eq. (32)). b) $\omega_c(k)$ is shown at $\Gamma_{\Delta} = 0.115$ GeV for different values of Fermi momenta $p_F = 280$, 290, 300, 360 MeV (curves 1, 2, 3, 4, correspondingly). For curves 3 and 4, the part of $\omega_c(k)$ on the physical sheet is drawn only. The curve 1 for $p_F = 280$ MeV is completely on the unphysical sheet.
- Fig. 5. The function $S/|\kappa(0)|$. a) Dependence of $S/|\kappa(0)|$ on the variation of nuclear parameters. Solid curve represents the main result obtained with $g'_{NN} = 1.0$, $g'_{N\Delta} = 0.2$, $g'_{\Delta\Delta} = 0.8$, $f_{\pi N\Delta} = 2.0$, $\Gamma_{\Delta} = 0.115$ GeV; the other parameters are described at the end of Sect. 3. Dashed curve corresponds to the calculation with $f_{\pi N\Delta} = 1.7$, dotted curve to $g'_{\Delta\Delta} = 1.2$, dot-dashed curve to $g'_{NN} = 0.7$. b) Dependence of $S/|\kappa(0)|$ on the isobar width. Solid curve represents the main result ($\Gamma_{\Delta} = 0.115$ GeV). Dotted curve corresponds to the calculation with $\Gamma_{\Delta} = 0.07$ GeV, dot-dashed curve to $\Gamma_{\Delta} = 0.05$ GeV, dashed curve to $\Gamma_{\Delta} = 0.01$ GeV.

- c) Dependence of $S/|\kappa(0)|$ on the behaviour type of $m^*(\rho)$. Solid curve stands for the result with m^* provided by Landau equation (6) $(m^*(\rho = \rho_0) = 0.8m)$. Dashed curve corresponds to Walecka equation (7) for m^* $(m^*(\rho = \rho_0) = 0.8m)$. Dot-dashed curve is obtained in framework of Walecka model, with $m^*(\rho = \rho_0) = 0.7m$.
- Fig. 6. Self-consistent results for the $\bar{q}q$ expectation value $\kappa(\rho)/|\kappa(0)| = \langle M|\bar{q}q|M \rangle/|\kappa(0)|$ (Eq. (2.1)) and $m^*(\rho)/m$ in nuclear matter. a) Dependence of $\kappa(\rho)/|\kappa(0)|$ on the variation of nuclear parameters. Scaling functions are $\beta=1, \alpha=\kappa(\rho)/\kappa(0)$. Solid curve is the main result obtained with $g'_{NN}=1.0, g'_{N\Delta}=0.2, g'_{\Delta\Delta}=0.8, f_{\pi N\Delta}=2.0$. Dashed curve corresponds to the calculation with $f_{\pi N\Delta}=1.7$, dotted one to $g'_{\Delta\Delta}=1.2$, dot-dashed curve to $g'_{NN}=0.7$. b) Dependence of $m^*(\rho)/m$ on the variation of nuclear parameters. Notation of curves are the same as in Fig. 6a. Straight line is drawn for the limit values of m^*/m (see the end of Sect. 5). Corresponding reliability limits for the calculation of $\kappa/\kappa(0)$ are marked by black points.
- Fig. 7. Self-consistent results for $\kappa(\rho)/|\kappa(0)|$ and $m^*(\rho)/m$ in the nuclear matter. a) Dependence of $\kappa(\rho)/|\kappa(0)$ on the type of scaling functions $\alpha(\rho), \beta(\rho)$. Solid curve displays the main result obtained with $\beta=1$, α is calculated by Eq. (37). Long-dashed curve corresponds to the gas approximation given by Eq. (1). For dotted curve $\beta=1, \alpha$ is taken from Eq. (38). For dot-dashed curve $\beta=1, \alpha$ is taken from Eq. (39). Dashed curve corresponds to the Brown-Rho scaling: $\beta=1/\alpha, \alpha=\kappa(\rho)/\kappa(0)$ (40). b) Dependence of $m^*(\rho)/m$ on the kind of scaling functions. Notations of the curves are the same as in Fig. 7a. Straight line is drawn for the limit values of $m^*(\rho)/m$ (see the end of Sect. 5). Corresponding reliability limits for the calculation of $\kappa/\kappa(0)$ are marked by black points.
- Fig. 8. Self-consistent results for $\kappa(\rho)/|\kappa(0)|$ and $m^*(\rho)/m$ with relativistic corrections. a) Dashed curve for $\kappa(\rho)/|\kappa(0)|$ is calculated with relativistic corrections (Sect. 6) and $\beta=1$, and $\alpha=\kappa/\kappa(0)$, Eq. (37). Dotted curve: $\beta=1$, and α is taken from Eq. (38). Dotdashed curve: $\beta=1$, and α taken from Eq. (39). Solid curve represents the main result $(\beta=1,\alpha=\kappa/\kappa(0))$, Eq. (37)) without relativistic corrections. b) The results for $m^*(\rho)/m$ calculated with relativistic corrections. Notations are the same as in Fig. 8a. Straight line restricts acceptable values of m^*/m from below, it is obtained using the same method as described above (see the end of Sect. 5) but with the isobar polarization operator, Eq. (46). Corresponding reliability limits for the calculation of $\kappa/\kappa(0)$ are marked by black points.
- Fig. 9. The graphical solution of the system of equations (47) and (48). a) The curves A1 and A2 are plotted for the equations (47) and (48), correspondingly, at certain small density ρ_A . The crossing points 1 and 2 are the two solutions of a system of equations. Dashed curves B1 and B2 correspond to the density value $\rho_B > \rho_A$. There is no solution in the latter case. b) Graphical solution of the set of equations (47) and (48), when baryon radius obeys the scaling equation (40). Solid curves A1 and A2 are plotted for Eqs. (47) and (48), correspondingly, at small ρ_A . There are three crossing points for solid lines, which are the three solutions of the system. Curves B1 and B2 are calculated at $\rho = \rho_B$, $\rho_B > \rho_A$. In this case only one solution survives.





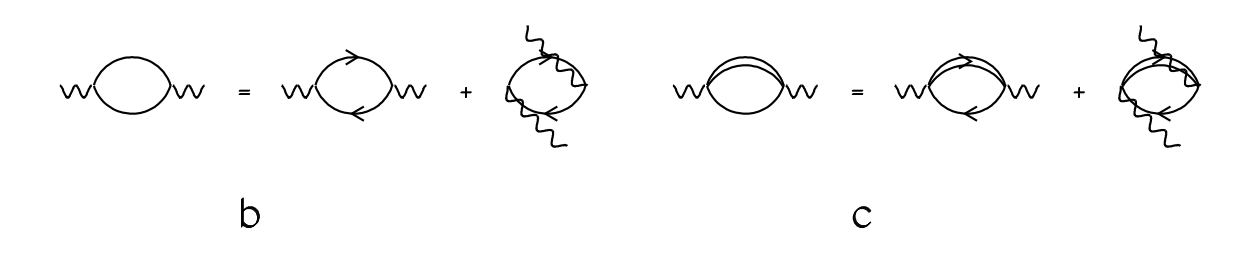


FIG. 2.

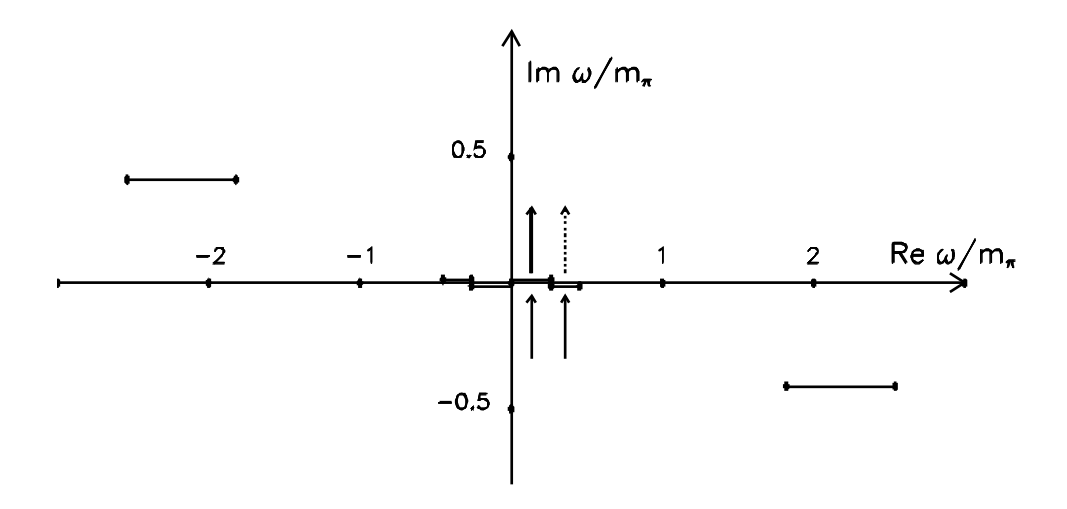


FIG. 3.

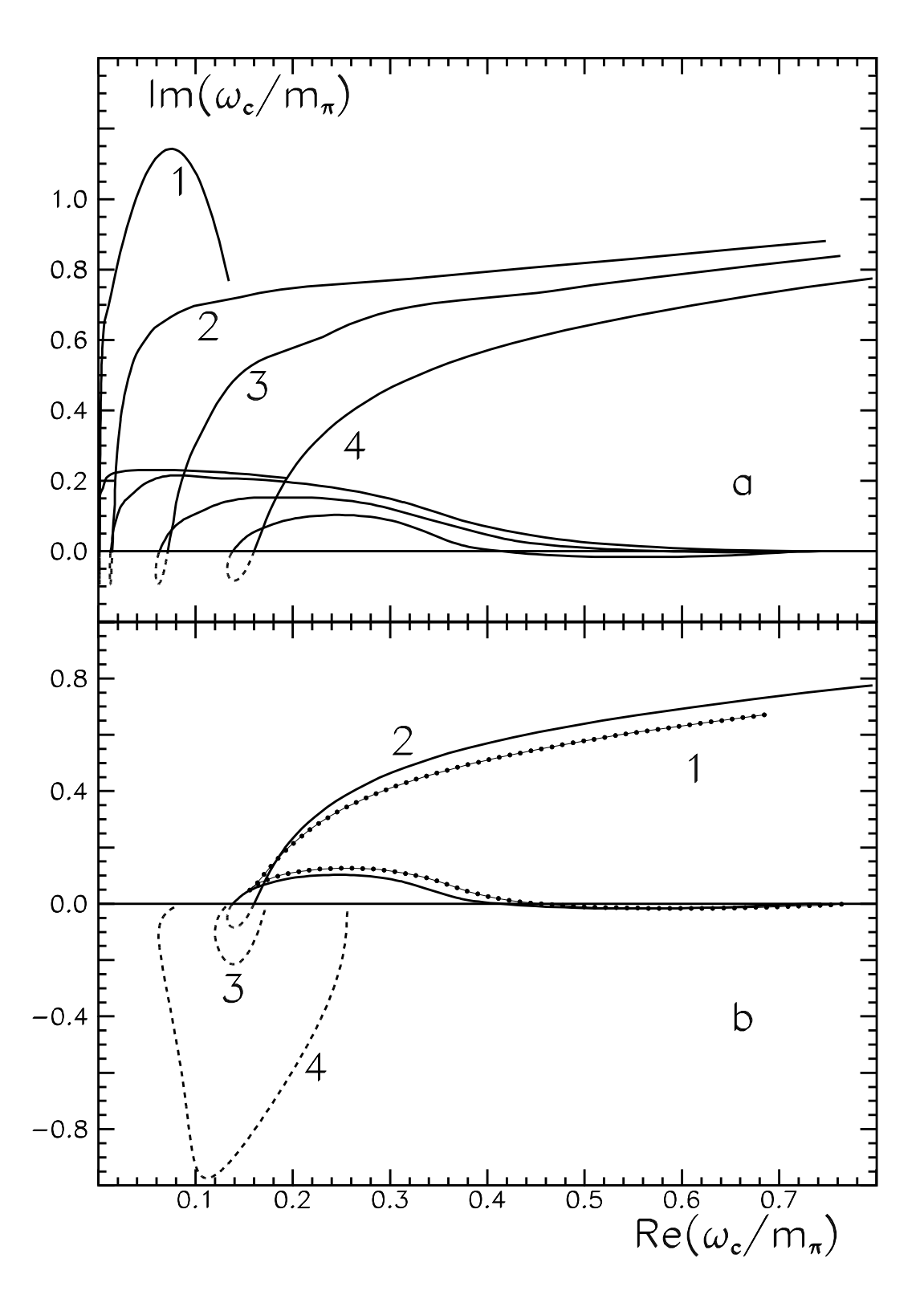


FIG. 4.

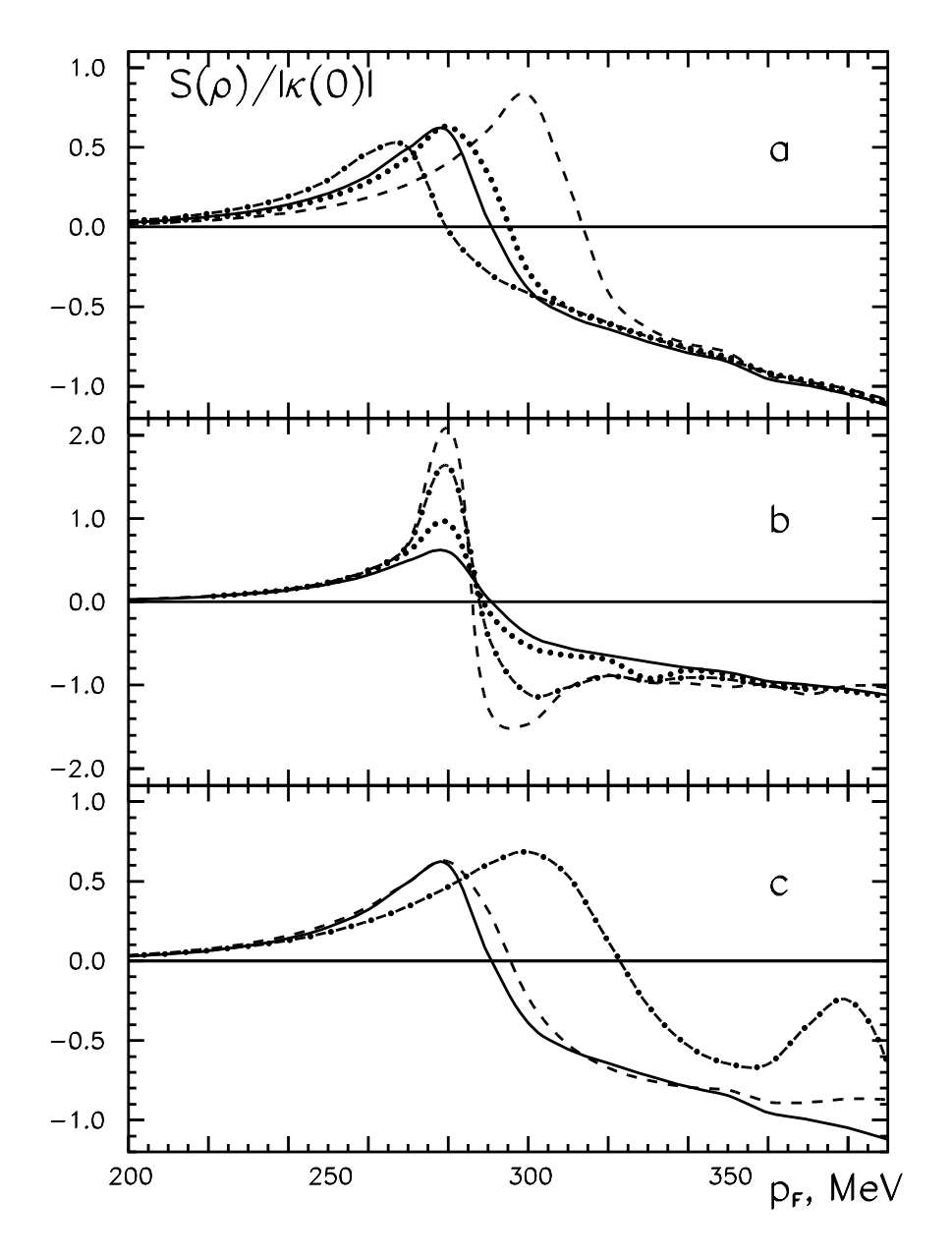


FIG. 5.

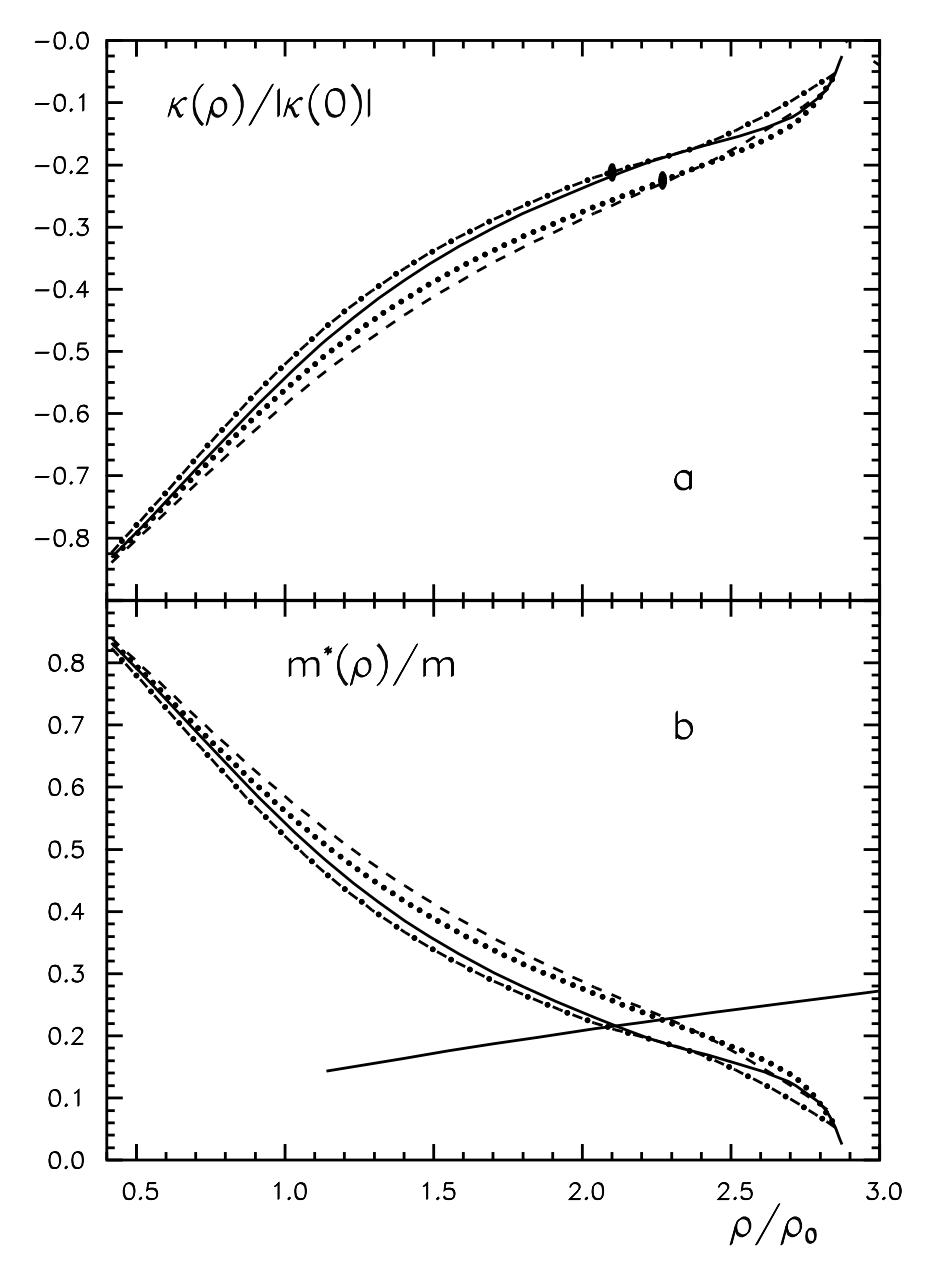


FIG. 6.

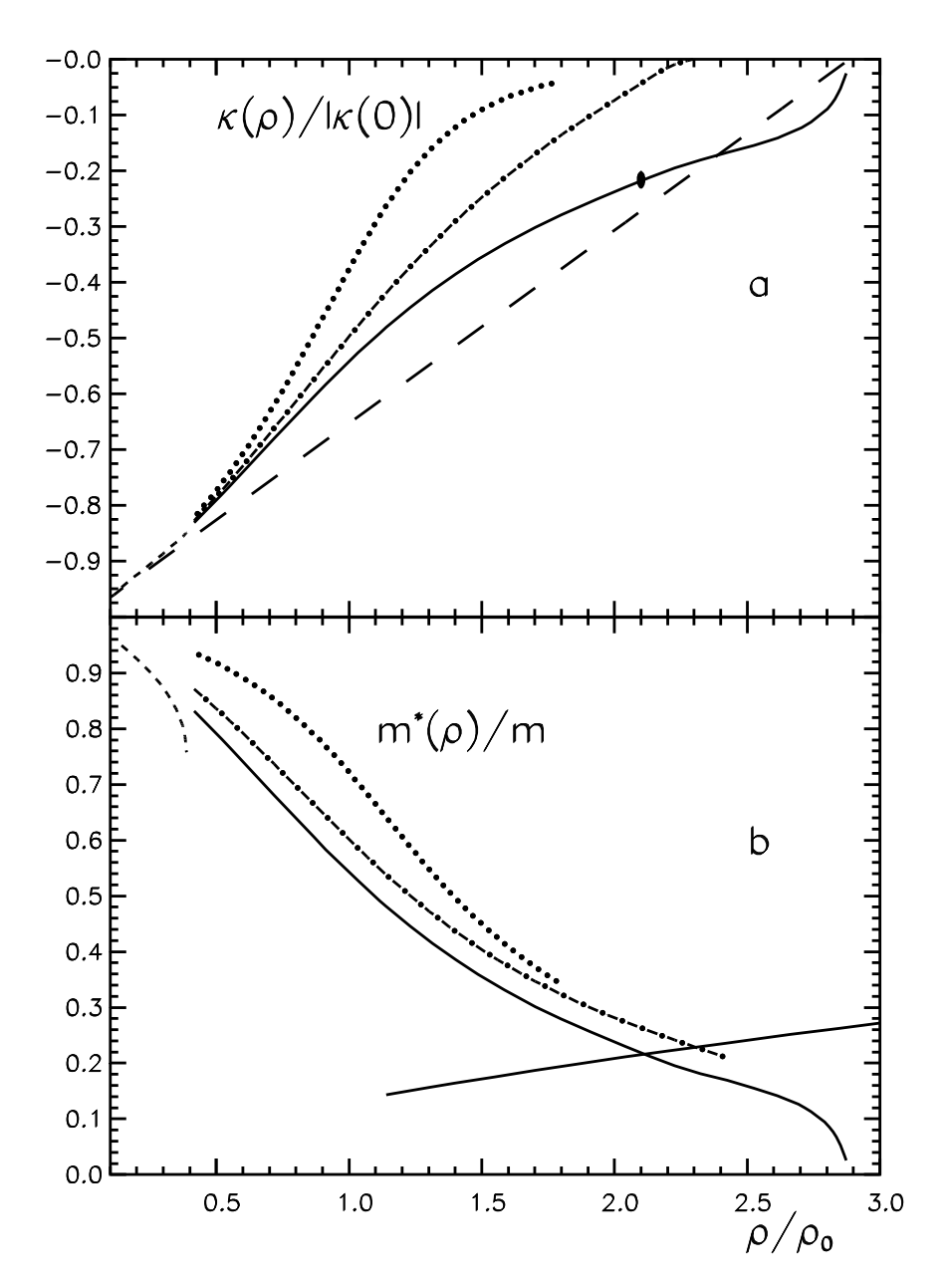


FIG. 7.

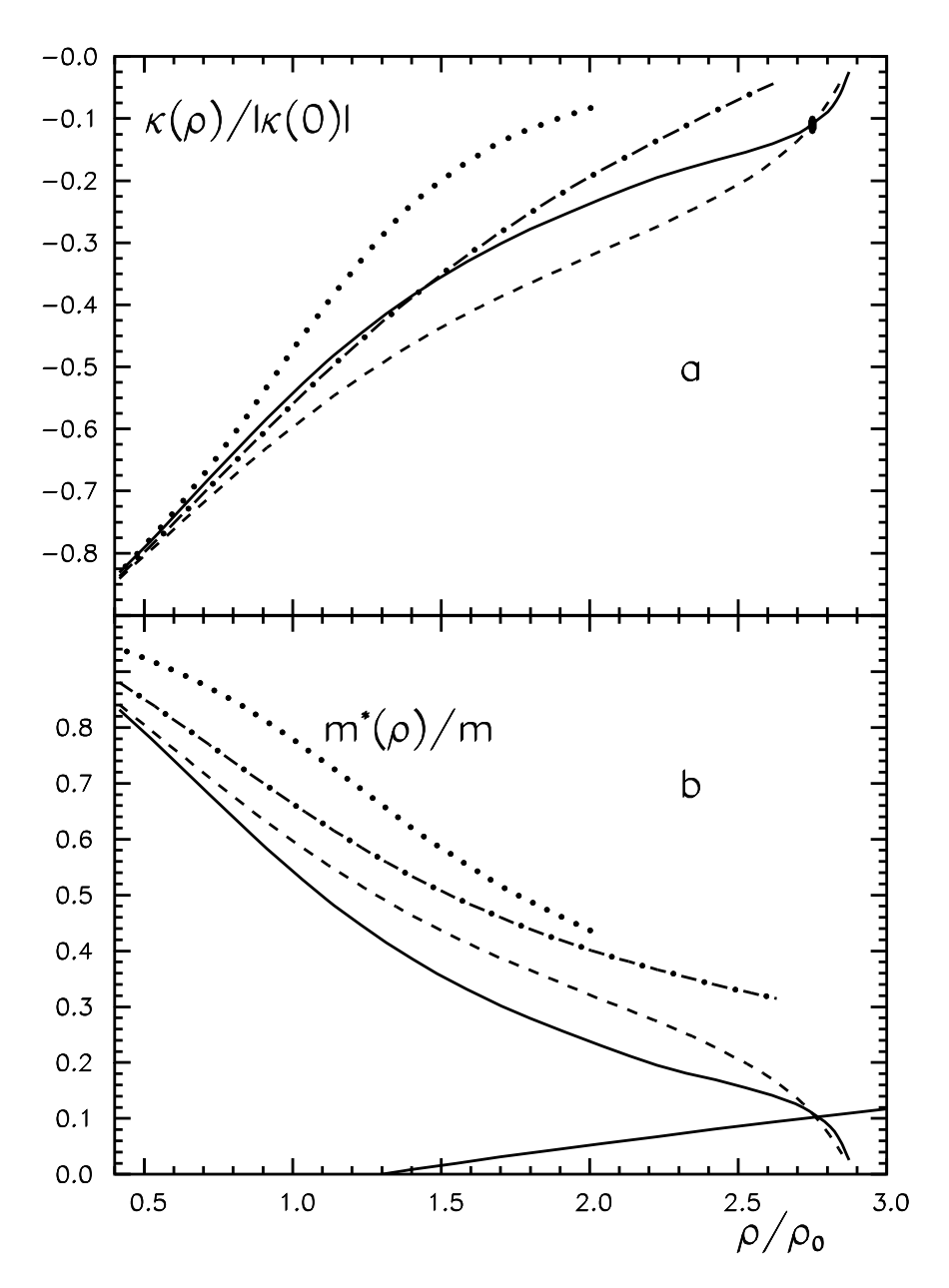


FIG. 8.

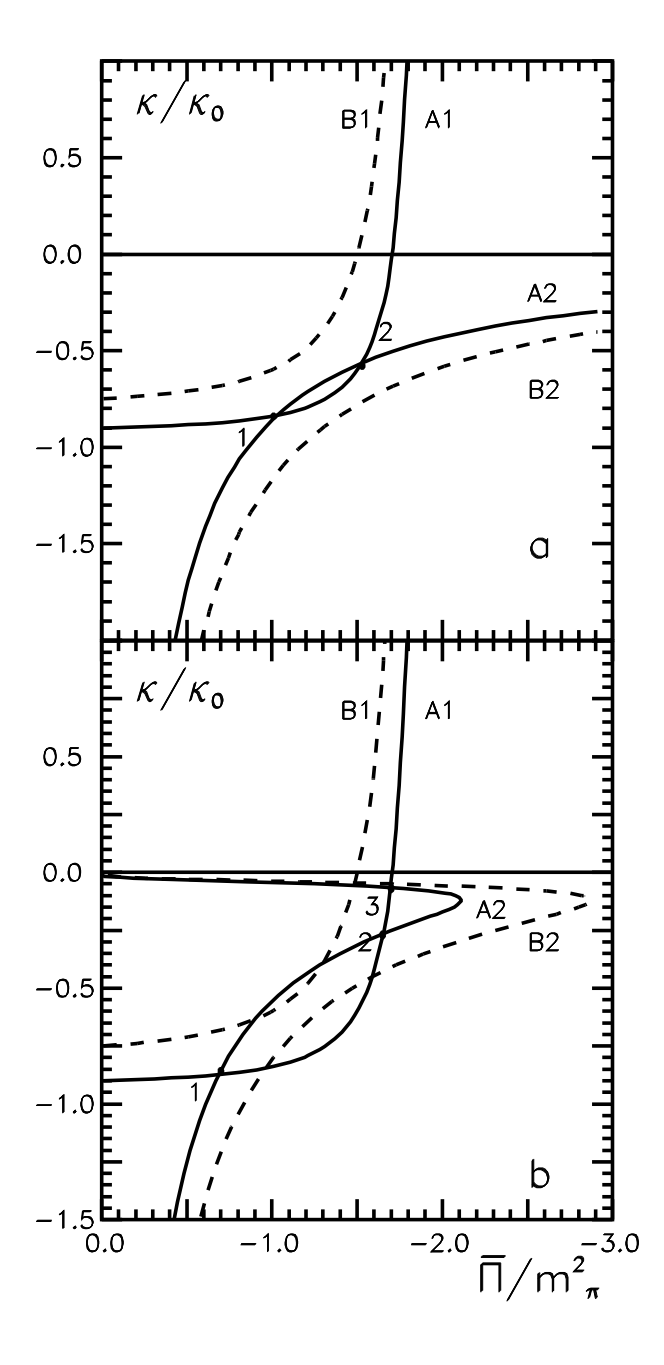


FIG. 9.